Dorottya Mészáros

Inter-Annual Morphometric Assessment of Fin whales (*Balaenoptera physalus*) Based on Drone Photogrammetry

UNIVERSIDADE DO ALGARVE

FACULDADE DE CIÊNCIAS E TECNOLOGIA

2023

Dorottya Mészáros

Inter-Annual Morphometric Assessment of Fin whales (*Balaenoptera physalus*) Based on Drone Photogrammetry

Master Thesis in Marine Biology

Internal Supervisor:
Catarina Vinagre PhD
University of Algarve

External Supervisor:
Eduard Degollada PhD
EDMAKTUB Association

UNIVERSIDADE DO ALGARVE
FACULDADE DE CIÊNCIAS E TECNOLOGIA
2023

Inter-Annual Morphometric Assessment of Fin whales (*Balaenoptera physalus*) Based on Drone Photogrammetry

Declaração de autoria de trabalho

Declaro ser a autora deste trabalho, que é original e inédito. Autores e trabalhos consultados estão devidamente citados no texto e constam da listagem de referências incluída.

Dorottya Mészáros

(signature**)**

Declaration of Authorship of work

I declare I am the author of this work, which is original and unpublished. The sources consulted have been duly cited in the text and included in the list of references.

Dorottya Mészáros

(signature**)**

Copyright

Copyright on behalf of Dorottya Mészáros, the University of Algarve

A Universidade do Algarve reserva para si o direito, em conformidade com o disposto no Código do Direito de Autor e dos Direitos Conexos, de arquivar, reproduzir e publicar a obra, independentemente do meio utilizado, bem como de a divulgar através de repositórios científicos e de admitir a sua cópia e distribuição para fins meramente educacionais ou de investigação e não comerciais, conquanto seja dado o devido crédito ao autor e editor respetivos

The University of Algarve reserves the right, in accordance with the provisions of the Code of the Copyright Law and related rights, to file, perpetual and without geographical limits, to archive and publicize this work through printed copies reproduced on paper or digitally, or by any other means known or to be invented, of disseminating it through scientific repositories and admit its copying and distribution for non-commercial educational or research purposes, provided that credit is given to the author and editor.

© Copyright: Dorottya Mészáros 2023

Abstract

Morphometrics such as length, body proportions, and volume are reliable data to determine the foraging success, energy reserve accumulation, and individual fitness, furthermore, it informs upon the population status of the examined species. Unmanned aerial vehicles (UAV) provides a new, low-cost, non-invasive platform to execute photogrammetric studies on free-ranging Cetaceans, enabling quantitative assessment of temporal and permanent changes of the animal's body. The aims of this study were to accumulate accurate morphometric measurements of fin whales (*Balaenoptera physalus*) in the Catalan coast, to compute growth trends of several body proportions, assess the evolution of body area index and body volume over time, and to compare these parameters within three consecutive foraging seasons. In total, 1099 still images were measured during this project, depicting 82 individual fin whales from three years between 2021 and 2023. The obtained results indicate that there were strong correlations among the growth trend of certain body parameters. The most significant correlation was between the total length of the body and the eye-to-eye distance. It was determined that in some cases the growth ratios can be further influenced by the gender and the size of the whale. Moreover, measures of three resighted individuals showed moderate increase of the body length and four animals showed gradual positive progression of the body area index and body volume within and over the three seasons, demonstrating foraging success and energy reserve accumulation. In a more general scale, smaller animals displayed the highest body area index, while the largest ones exhibit the lowest measures. The present study illustrates the utility of drone-based photogrammetry to detect and assess temporal and permanent changes in the body parameters of fin whales in the Garraf coast.

Keywords: morphometric assessment, body volume, body area index, body proportions, growth trends, photogrammetry, fin whale, UAV

Resumo

Todos os anos, as baleias-comuns (*Balaenoptera physalus*) reúnem-se ao longo da costa Catalã no Mar das Baleares, entre fevereiro e junho, para se alimentarem. Este evento constitui uma oportunidade para recolher dados e estudar estes misticetes pelágicos de vida livre, mais perto da costa. As baleias-comuns são uma parte substancial da teia alimentar, pois não são apenas consumidores de biomassa, mas também promotores da produção primária, reciclando grandes quantidades de nutrientes e aumentando assim a capacidade de carga dos ecossistemas. Além disso, a energia obtida durante as épocas de procura de alimento é armazenada em lípidos e utilizada durante o período de migração e reprodução. Por conseguinte, a monitorização da taxa/tendência de crescimento e das alterações no perfil da forma e nas proporções corporais fornece uma visão da aptidão física, da resiliência, do sucesso da procura de alimento e, com isso, do estado nutricional. Além disso, numa escala maior, oferece uma visão do estado da população e da dinâmica populacional. Além disso, as alterações temporais na sua morfometria fornecem informações sobre as condições, a produtividade e a capacidade de carga do ecossistema de suporte.Para a realização do projeto foi utilizada a fotogrametria aérea, que é um novo método seguro, não invasivo e económico na investigação de cetáceos. A técnica permite a observação de uma perspetiva vertical com um veículo aéreo não tripulado (VANT) para obter um conjunto de dados e executar medidas morfométricas corporais precisas no programa chamado MorphoMetriX para avaliação quantitativa. As análises de várias métricas fornecem informações sobre o desenvolvimento do corpo e facilitam a evidência da resposta fisiológica às mudanças ambientais. O conhecimento/banco de dados compilado pelo método pode ser útil em termos de gestão populacional e em ações de conservação.Os objetivos deste projeto foram acumular medidas morfométricas precisas, como comprimento, largura e proporção de baleias-comuns na costa Catalã para calcular as tendências de crescimento de vários parâmetros e proporções corporais, avaliar a evolução do índice de área corporal e do volume corporal ao longo do tempo para visualizar mudanças no armazenamento de energia e comparar esses parâmetros em três temporadas consecutivas de alimentação na costa Catalã. Deste modo, melhorando o conhecimento da única especie de baleia de barbas que está presente durante todo o ano, no Mar Mediterrâneo.

Para este estudo, foi analisado um total de 366 filmagens aéreas (2021: 193, 2022: 109, 2023: 67), das quais 1099 imagens fixas foram medidas no MorphoMetriX para obter medidas fotogramétricas precisas e fiáveis, retratando 82 baleias-comuns individuais ao longo dos três anos. A maioria dos animais encontrados tinha entre 14 e 19 metros de comprimento. Foram

obtidos nove atributos morfométricos com base nas medidas padrão dos parâmetros corporais das baleias descritas por Ratnaswamy & Winn em 1993, a partir das quais foram calculadas quinze comparações proporcionais. Foi criada uma matriz de correlação para prever a relação entre os parâmetros corporais medidos. Foram desenvolvidos vários modelos lineares para investigar a interdependência do crescimento entre partes do corpo fortemente correlacionadas. Para além disso, a largura do corpo foi medida em incrementos de 20% ao longo do comprimento do corpo inteiro. A partir desses valores, o índice de área corporal e o volume corporal foram calculados para avaliar as alterações na reserva de energia dos indivíduos durante as épocas de alimentação e para comparar o sucesso de alimentação dos três anos. O resultado indica que existem fortes correlações entre a tendência de crescimento de certos parâmetros corporais. A interdependência mais significativa verificou-se entre o comprimento total do corpo e a distância olho-a-olho. Além disso, o crescimento das extremidades, nomeadamente a barbatana dorsal e a barbatana caudal, também apresentou uma forte ligação. Com base em modelos lineares, determinou-se que, em alguns casos, os rácios de crescimento podem ser ainda mais influenciados pelo sexo e pelo tamanho da baleia. Além disso, as medidas de três indivíduos reavistados mostraram um aumento moderado do comprimento do corpo e quatro animais mostraram uma ligeira progressão do índice de área corporal e do volume do corpo durante as três estações, o que demonstra o sucesso da procura de alimentos e a acumulação de reservas energéticas. Numa escala mais geral, os animais mais pequenos apresentaram o índice de área corporal mais elevado, enquanto os maiores exibiram as medidas mais baixas. Com base nestas duas medidas (BAI, BV), foi possível descobrir variações na produtividade da área entre os três anos. Em comparação com as duas primeiras épocas examinadas, 2023 foi significativamente superior, enquanto 2021 e 2022 a média da medida do volume corporal foi estatisticamente igual. No entanto, existe incerteza nas medidas fotogramétricas devido à medição da altitude dos drones com base no GPS, que neste caso obteve um "erro fotogramétrico médio" de 2,5% no caso do Mavic Pro 2 e de 9,8% no caso do Mavic 3.

A fotogrametria baseada em drones provou ser um método preciso para monitorizar as tendências de crescimento e as alterações da condição corporal das baleias-comuns na costa de Garraf, para reduzir as incertezas do estado nutricional e do desenvolvimento corporal. Foi uma caraterística importante do estudo associar baleias individuais a medições obtidas por fotogrametria, o que permitiu monitorizar alterações nos parâmetros corporais ao longo do tempo. No entanto, tal só foi possível no caso de seis animais, devido a dificuldades de recolha de imagens adequadas e ao limite de tempo, independentemente do método. No entanto, todas

estas baleias registaram um aumento geral do comprimento, cujos resultados se distribuíram uniformemente ao longo dos três anos analisados. Para além disso, a avaliação da condição corporal (BV, BAI) dos indivíduos também resultou num aumento moderado durante a época. Além disso, a comparação inter-anual das medidas de BAI forneceu uma visão da produtividade e da capacidade de carga da área, mostrando o desvio na disponibilidade de presas.

Estes resultados ajudam a preencher as lacunas de conhecimento sobre as populações de baleias-comuns que surgem na costa de Garraf, esta técnica tem potencial para realizar uma monitorização a longo prazo para acumular dados que permitam obter resultados mais fiáveis sobre a relação entre parâmetros corporais, tendências de crescimento, alterações nas condições corporais e dinâmica populacional. Este conhecimento pode ser útil para estabelecer acções de conservação e gestão populacional adequadas para proteger a zona de alimentação dentro da área, a fim de manter um abastecimento alimentar adequado para as baleias-comuns migratórias. Por conseguinte, a continuação de tais estudos é altamente recomendada e necessária para obter resultados mais representativos.

Keywords: morphometric assessment, body volume, body area index, body proportions, growth trends, photogrammetry, fin whale, UAV

Table of Contents

List of abbreviations, acronyms, and symbols

UAV: Unmanned Aerial Vehicle

TL: total length (from the tip of the rostrum, until the notch of the fluke)

FS: fluke spread

SB: distance from the snout to blowhole

SD: snout to dorsal fin

SAF: distance from snout to anterior insertion of the flipper

SPF: distance from snout to posterior insertion of the flipper

AFL: anterior flipper length

PFL: posterior flipper length

ETE: width between the eyes

BAI: body area index

BV: body volume

1. Introduction

Fin whales (*Balaenoptera physalus*) are the second largest of the baleen whales, with slender bodies reaching approximately 18 to 27 meters in length (Aguilar *et al.*, 1987). However, in the Northern Hemisphere Fin whales tend to grow smaller than in the Southern Hemisphere (Jefferson *et al*., 2015). In general females grow larger than males (Aguilar & Gracía-Vernet, 2018), with about 5-10% of the total length (Jefferson *et al*., 2015). The species is recognizable by its asymmetric coloration of the head, where the right side of the dorsal part has a lighter grayish-whitish color that even extend to the ventral side of the head as the blaze pattern (Fig. 1.1) (Degollada *et al*., 2023).

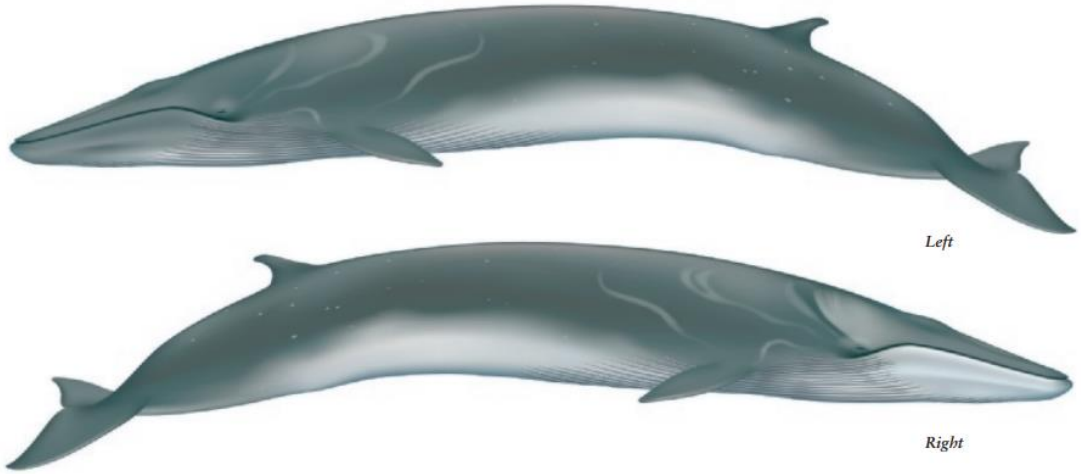

Figure 1.1- Fin whale Morphology (Jefferson *et al*., 2015)

Fin whales are a free-ranging, pelagic species with a worldwide distribution (they can be found in all oceans). It is a migratory species that shows an annual migratory pattern between subpolar and temperate feeding grounds and the warmer breeding grounds in the subtropics, tropics (Figure 1.2.) (Notrabar *et al.*, 2003). They are the only baleen whales present year-round in the Mediterranean Sea (Castellote *et al*., 2012; Degollada *et al*., 2023). Similarly, to other mysticetes fin whales feed on a wide range of invertebrates, such as planktonic crustaceans, as well as on schooling fish. The prey species vary amongst Hemispheres, locations, seasons and further depend on availability (Notrabar *et al.*, 2003).

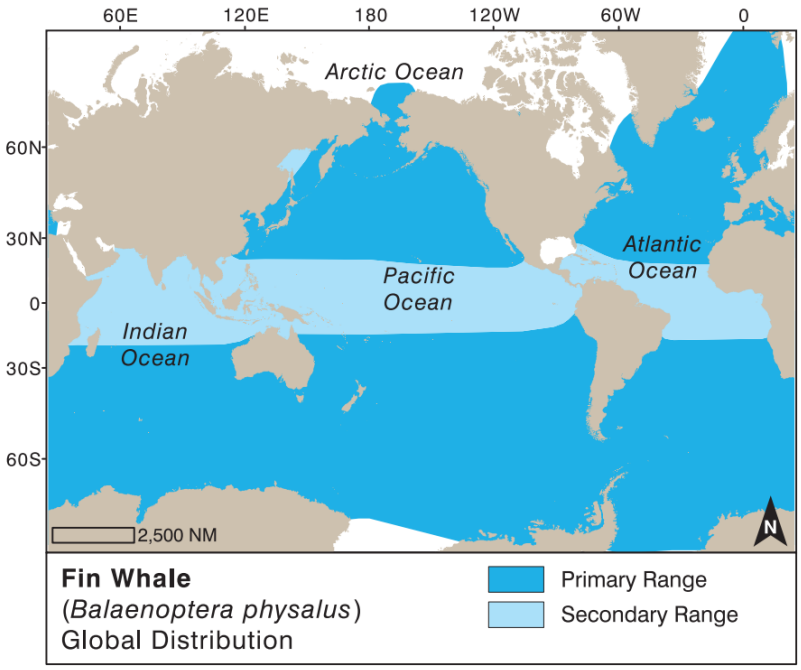

Figure 1.2- Fin whale distribution (Jefferson *et al.*, 2015).

Due to this large-scale movement and the different nutritive condition of the animals, there is a seasonal transformation/variation in the relative body mass (Aguilar & Gracía-Vernet, 2018). Every feeding season the animals need to accumulate a sufficient amount of energy reserve to achieve higher fitness, survival rate, breeding success and resilience against changing environmental factors. The adequate amount of energy storage varies between genders, age groups, and reproductive status (Aoki *et al.*, 2021). Accordingly, the relative amount of energy storage (body condition) is an indicator of the whale's fitness (Castrillon & Bengstone Nash, 2020). The energy is stored as lipids in fat and blubber. Lipids have lower tissue density; therefore, these tissues take up more space as they have higher volume than muscle for example. Based on this, individuals with higher reserves have an overall higher body volume and body area, which is visible in the width of the animal (Aoki *et al.*, 2021) and in the shape profile (Durban *et al.*, 2016) compared to the given body length. Therefore, the external body shape is an accurate indicator of the body condition (Aoki *et al.*, 2021). The changes of the amount of energy storage can be measured and monitored by calculating the body volume and the body area index (which is a continuous, scale-invariant and unitless measure) (Soledade *et al.*, 2020) as both of these metrics correlate with the lipid content of the animal's body (Hirtle *et al.*, 2022).

Furthermore, growth is also an important factor and a reliable attribute which gives an insight of the individual's age, sexual maturity and of the population status (Durban *et al.*, 2016). Adult

body size is (which is approximately 95% of the final size) reached approximately between the age 9 and 13. Afterwards, the animal still grows slowly but continuously until reaching physical maturity (ossification of the vertebrates), which occurs around the age of 25 (Aguilar & García-Vernet, 2018).

Today's technology allows an inexpensive, non-invasive method to conduct indirect physical body measurements (Dawson *et al*., 2017; Castrillon *et al*., 2020; Aoki *et al.*, 2021; Cheney *et al*., 2022; Degollada *et. al*., 2023) of free ranging cetaceans by implementing a different perspective (Burnett *et al.*, 2019). Unmanned aerial vehicle (UAV) is widely used in the field of cetacean research, enabling it to collect vertical footage and images. With the help of UAVs aerial photogrammetry can be conducted (Dawson *et al*., 2017; Aoki *et al*., 2021), which is the method of processing video footage, measuring the object and interpreting the obtained still images (Aber *et al*., 2019). To this technique morphometric measurements are successfully adapted, which is a measuring technique that quantifies an objects morphological characteristics, such as size, shape and proportions (Rohlf, 1990; Castrillon & Bengtson Nash, 2020).With this method, temporal changes in the body morphology (such as the body shape profile) and growth trends can be followed over time, which gives information upon individual foraging success, fitness, energy storage, furthermore the population status and indirectly even the condition of the ecosystem of the habitat (Castillon & Bentson Nash, 2020).

1.1 References

Aber J., Marzolff I., Ries J., Aber S. (2019). *Small-Format Aerial Photography and UAS Imagery, Chapter 3, Second Edition, Elsevier, Amsterdam. ISBN: 9780128129432, pp 23-39.*

Aguilar A., & García-Vernet R. (2018). *Fin Whale. Wursig B., Thewissen J. G. M., Kovacs K. Encyclopedia of Marine Mammals, Third Edition, Academic press, Cambridge, Massachusetts. ISBN: 9780128043813, 368–371pp.*

Aguilar A., Lockyer C. H. (1986). *Growth, physical maturity, and mortality of fin whales (Baleanoptera physalus) inhabiting the temperate waters of the northeast Atlantic. Canadian Journal of Zoology, 65, 253-264pp.*

Aoki k., Isojunno S., Bellot C., Iwata T., Kershaw J., Akiyama Y., Martín Lopez L., Ramp C., Biuw M., Swift R., Wensveen P., Pomeroy P., Narazaki T., Hall A., Sato K., Miller P. (2021). *Aerial photogrammetry and tag-derived tissue density reveal patterns of lipid-store body condition of humpback whales on their feeding grounds. Proceedings of the Royal Society B: Biological Sciences, 288, 1-10pp.*

Burnett, J. D., Lemos, L., Barlow, D., Wing, M. G., Chandler, T., & Torres, L. G. (2019). *Estimating morphometric attributes of baleen whales with photogrammetry from small UASs: A case study with blue and gray whales. Marine Mammal Science, 35(1), 108-139pp.*

Castellote M., Clark C., Lammers M. (2012). *Fin whale (Balaenoptera physalus) population identity in the western Mediterranean Sea. Marine Mammal Science, 28(2), 325-344pp.*

Castrillon J., Bengtson Nash S., (2020). *Evaluating cetacean body condition; a review of traditional approaches and new developments. Ecology and Evolution,10(12), 6144-6162pp.*

Cheney B., Dale J., Thompson P.,Quick N. (2022). *Spy in the ksy: a method to identify pregnant small cetaceans. Remote Sensing in Ecology and Conservation 8(4), 492-505pp.*

Dawson S., Bowman M., Leunissen E., Sirguey P. (2017). *Inexpensive Aerial Photogrammetry for Studies of Whales and Large Marine Animals. Frontiers in Marine Science, 4(), 366-373pp.*

Degollada E., Amihó N., O'Callaghan S. A., Varola M., Ruggero K., Tort B. (2023). *A Novel Technique for Photo-Identification of the Fin Whale, Balaenoptera physalus, as Determined by Drone Aerial Images. Drones, 7(3), 220-pp.*

Durban J., Moore M. J., Chiang G., Hickmott L. S., Bocconcelli A., Howes G., Bahamonde P. A., Perryman W. L., LeRoi D. J., (2016). *Photogrammetry of blue whales with an unmanned hexacopter. Marine Mammal Science, 32(4), 1510-1515pp.*

Jefferson T. A., Webber M. A., Pitman R. L. (2015). *Marine Mammals of the Word: A Comprehensive Guide to Their Identification, Academic press, Cambridge, Massachusetts. ISBN: 978-0-12-409542-7, 54-58pp.*

Hirtle N., Stepanuk J., Heywood E., (2022). *Integraing 3D models with morphometric measurements to improve volumetric estimates in marine mammals. Methods in Ecology and Evolution, 13(11), 2478-2490pp.* https://doi.org/10.1111/2041-210X.13962

Notarbar Tollo-di-sciar G., Zanardelli M., Jahoda M., Panigada S., Airoldi S. (2003). *The fin whale BAlenoptera physalus (L. 1758) in the Mediterranean Sea. Mammal Review, 44(2), 105-150pp.*

Soledade Lemos, L., Burnett, J. D., Chandler, T. E., Sumich, J. L., & Torres, L. G. (2020). *Intra- and inter-annual variation in gray whale body condition on a foraging ground. Ecosphere, 11(4).*

Rohlf F. J. (1990). Morphometrics. *Annual Review of Ecology and Systematics*, 21(1), 299-316.

Inter-Annual Morphometric Assessment of Fin whales (*Balaenoptera physalus*) Based on Drone Photogrammetry

Dorottya Mészáros

University of Algarve

a47304@ualg.pt

Keywords: morphometric assessment, body volume, body area index, body proportions, growth trends, photogrammetry, fin whale, UAV

Abstract

Data upon the animal's body such as length, proportions, and volume are reliable metrics to determine the foraging success, energy reserve accumulation, individual fitness and furthermore the informs upon the population status of the examined species, the fin whale. Unmanned aerial vehicle (UAV) provides a new, low-cost, non-invasive platform to execute photogrammetric studies on free-ranging Cetaceans, enabling quantitative assessment of temporal and permanent changes of the animal's body. The aims of this study were to accumulate accurate morphometric measurements of fin whales in the Catalan coast to compute growth trends of several body proportions, asses the evolution of body area index and body volume over time, and to compare these parameters within three consecutive foraging seasons. In total 1099 still images were measured during this project, depicting 82 individual Fin whales from three consecutive years, between 2021 and 2023. The result indicates that there are strong correlations among the growth trend of certain body parameters. The most significant correlation was between the total length of the body and the eye-to-eye distance. It was determined that in some cases the growth ratios can be further influenced by the gender and the size of the whale. Moreover, measures of three resighted individuals showed moderate increase of the body length and four animals showed gradual positive progression of the body area index and body volume within and over the three seasons, demonstrating foraging success and energy reserve accumulation. In a more general scale, smaller animals displayed the highest body area index, while the largest ones exhibit the lowest measures. The present study illustrates the utility of drone-based photogrammetry to detect and assess temporal and permanent changes in the body parameters of fin whales in the Garraf coast.

Keywords: morphometric assessment, body volume, body area index, body proportions, growth trends, photogrammetry, fin whale, UAV

2. Introduction

Fin whales are a free-ranging, pelagic species with a worldwide distribution (they can be found in all oceans) (Notrabar *et al*., 2003). Besides, it is the only baleen whale species present year-round in the Mediterranean Sea (Castellote *et al*., 2012; Degollada *et al*., 2023).

Just as other mysticetes Fin whales are migratory species that show an annual movement pattern between subpolar and temperate feeding grounds and the warmer breeding grounds in the subtropics, tropics (Notrabar *et al*., 2003). Due to this large-scale movement and the different nutritive conditions the animals show seasonal variation in the relative body mass (Aguilar & Gracía-Vernet, 2018). Every feeding season the animals need to accumulate a sufficient amount of energy reserve to achieve higher fitness, survival rate, breeding success and resilience against changing environmental factors (Soledade *et al*., 2020). The adequate amount of energy storage varies between genders, age groups, and reproductive status (Castrillon & Bengtson Nash 2020; Soledade *et al*., 2020; Aoki *et al*., 2021). Accordingly, the relative amount of energy storage (body condition) is an indicator of the whale's fitness (Christiansen *et al*., 2019; Castrillon & Bengstone Nash, 2020; Soledade *et al*.), survival and reproductive success; moreover, it provides information upon the life history on an individual and population level (de Oliveira *et al*., 2022). Furthermore, the growth is also an important factor and a reliable attribute which gives an insight of the individuals age, sexual maturity and of the population status (Durban *et al*., 2016).

Therefore, by investigating the annual or seasonal variation of Fin whales, morphometric attributes are an extremely useful way to obtain data that represents the health, energetic gains, and costs of these animals (Shero *et al*., 2014), which is highly associated with the reproduction and feeding periods (de Oliveira *et al*., 2022). However, it is challenging to study this cetacean species as they are free-ranging and pelagic. In recent years unmanned aerial vehicles created a new, safe, low-cost technique to obtain accurate and reliable (by including several sensors) data (de Oliveira *et al*., 2022). With this method, temporal changes in the body morphology (such as the body shape profile) and growth trends can be followed over time, which gives information upon individual foraging success, fitness, energy storage, furthermore the population status (Castillon & Bentson Nash, 2020) and it also acts as an indicator of food availability in the area (Shero *et al*., 2014).

The aims of this study were to accumulate accurate morphometric measurements of fin whales (*Balaenoptera physalus*), in the Catalan coast to compute growth trends of several body

proportions, assess the evolution of body area index and body volume over time, and to compare these parameters within three consecutive foraging seasons between 2021 and 2023.

3. Material and Methods

3.1 Study Area

The research was conducted in a geographically distinct foraging ground situated in the Western Mediterranean, in the Spanish coastline, approximately between Barcelona and Tarragona in the Balearic Sea (Degollada *et al*., 2022). This area is between two rivers, Ebro (Lloret *et al*., 2003) and Llobregat which are coming from the North of Spain and affecting the primary production greatly within the study area with their nutrient input (Rigual-Hernández *et al*., 2010). Besides two submarine canyons can be found in this range, the Cunit and Foix canyons which further affects the prey availability due to upwelling (Tort *et al*., 2022). This area covers about 1944 km^2, usually 12-15 miles from the shore (Figure 3.1) (Degollada *et al*., 2022).

Data collection was conducted in three foraging seasons between 2021 and 2023, from February to June. During this time of the year fin whale populations migrate to this area to feed from various locations (Degollada *et al*., 2022, Tort *et al*., 2022), however yet unknown (Castellote *et al*., 2011; Degollada et. al., 2020). Based on observations and studies from the previous years it has been hypothesized by the research association EDMAKTUB, that animals both from the Atlantic Ocean and from the Mediterranean Sea are present in the Catalan coast during the foraging seasons (Degollada *et al*., 2022).

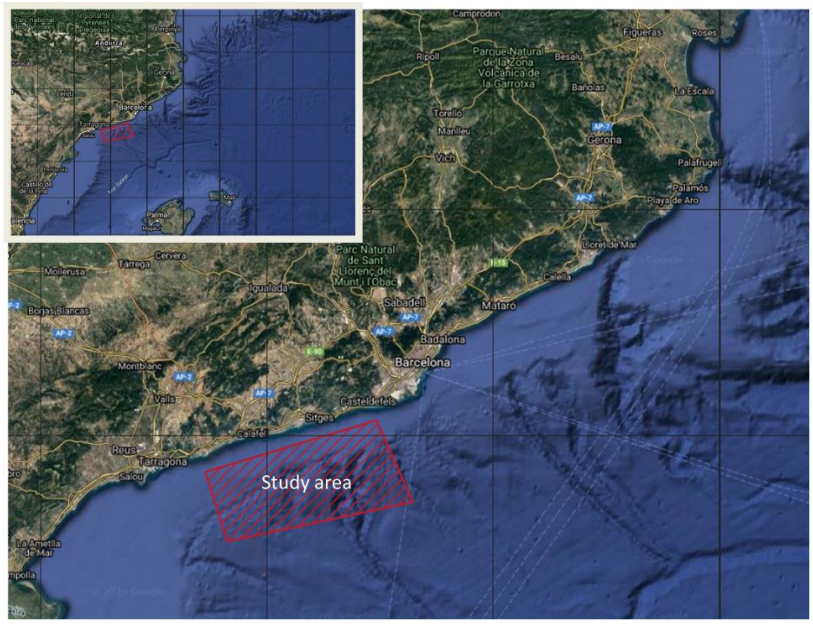

Figure 3.1- Satellite Picture of the study area (provided by EDMAKTUB)

3.2 Data collection

The field work was conducted (under the following permission: Ref: SGBTM/BDM/AUTSPP/21/2022 and SGBTM/BDM/AUTSPP/20/2023) on board of EDMAKTUB non-profit organization's research vessel, MAKTUB a 14.15 meter long, well equipped catamaran. The boat was kept at the sailing club in Vilanova i la Geltrú, from where the research trips have started. In the course of each trip the environmental conditions (sea state, swell heights, cloud coverage, visibility, precipitation) and information upon the boat (depth, boat course and velocity, if the engine is on or sailing, and activity of the researchers on board) are recorded in Logger2010 (version 5.0) every 30 minutes. On the sea, after the whales are sighted the boat switches from sail to engine (under 5 knots) to approach the animal following the regulations (Real Decreto 1727/2007). Simultaneously, for the sighting the environmental conditions are being saved in Logger2010 furthermore, the time, sighting site (bow, starboard, port, stern) the angle, the animal's position, animal's direction, species name, the cameras and drone that was used for photo-ID and behavioral data was recorded on a sighting sheet. When the whale is approximately between 100–300-meter range, the boat turns and moves parallel to the animal. Besides, when it was possible life-history traits were assessed visually by the researchers on board (Degollada *et al.*, 2023).

If the weather conditions were adequate (swell less than 2 meters, wind speed less than 10 meter per second) a Mavic 2 Pro UAV and/or a Mavic 3 was launched from the deck (stern) to collect video records for whale photogrammetry and for photo-identification (Degollada *et al.*, 2023). The UAS was remotely operated from the vessel using the DJI application on an Apple iPad, following the protocol described by Degollada *et al*. from 2023. The base lines for recording the footage for photogrammetry were the following: to keep the device over the whale while it was surfacing ("sample points") (Hartman *et al*., 2020), with the camera pointing down at the animal, while keeping the whale in the center of the field of view (Soledade *et al.*, 2020). Arial videos were taken of the Fin whales and at the same time behavioral data was noted down in PADOC application (version 4.3002) to observe if there is any response to the drone presence (Soledade Lemons *et al.*, 2020). Furthermore, to provide a scale of measurements and to calibrate the accurate altitude (Best & Ruther, 1992; Torres & Bierlich, 2020) aerial videos were captured of a calibration object with known length (Dawson *et al*., 2017), in this case of a kayak between 100- and 10-meter altitudes with 10-meter increments (Bierlich *et al*., 2021).

3.3 Data Analysis

3.3.1 Photo-identification

Photographs were obtained of the animals, especially of the dorsal fin from both sides (Aoki *et al*., 2021) by two digital SLR cameras (Nikon D7100 with AF-S 75-300 VR Nikon lens and another Nikon D7100 with 150-600 Sigma lens) and aerial images of the chevron and the blaze with the drones for photo-identification (Degollada *et al.*, 2023).

The photographs captured from the deck with the digital cameras during field survey and images obtained from the drone videos were visually assessed, firstly the quality of the images (focus, angle, glare, etc.). Thereafter, the photographs that met the expectations (good quality) went under a second visual inspection (Soledade Lemons *et al*., 2020), where the shape of the dorsal fin, unique marks, nicks, parasites, lesions and skin pigmentations especially the central chevron pattern (behind the head on the dorsal side a unique V-shaped coloration) and the blaze (Figure 3.2) were checked in the depicted whale, based on which individual animals can be recognized with the help of the Fin whale photo-id catalog created by EDMAKTUB (Degollada *et al*., 2023). When adequate footage was obtained of the same sighting the identified animals

were matched from both methods (UAV, general camera-based photo-ID) (Cheney *et al.*, 2022). If possible, the sex was determined based on previously collected biopsy samples.

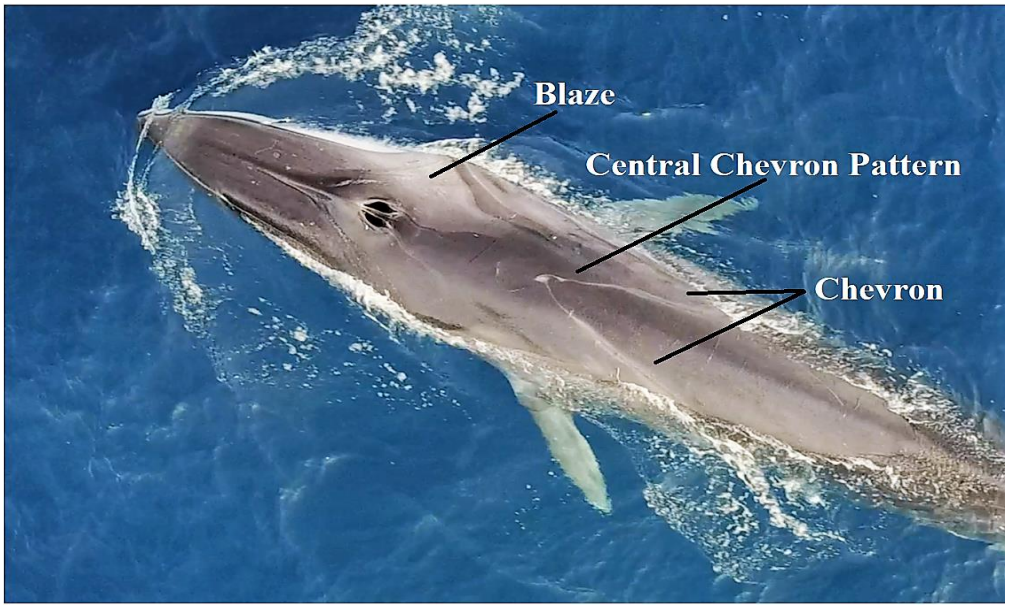

Figure 3.2- Unique pigmentation pattern (blaze, chevron, central chevron pattern) of Fin whales (*Balaenoptery physalus)* viewed from aerial photogrammetry. Photograph by EDMAKTUB Association.

3.3.2 Photogrammetry

Firstly, the flight record was converted into a csv. file using the DJI Flight Log Viewer from phantomhelp.com website. Then in each flight record csv. files the recorded footage was searched by checking the "CAMERA.isVideo" column to know when the drone recording was and matching it with the flight time from the "OSD.flyTime" column (Figure 3.3). In an excel sheet called "matched_drone_records" the row number where the video begins and ends were noted down with the corresponding flight time, from which the length of each video is calculated. Subsequently, when a whole day's recordings were collected in the excel sheet the actual footage from that day were matched to the adequate video from the flight record by their length (Figure 3.4).

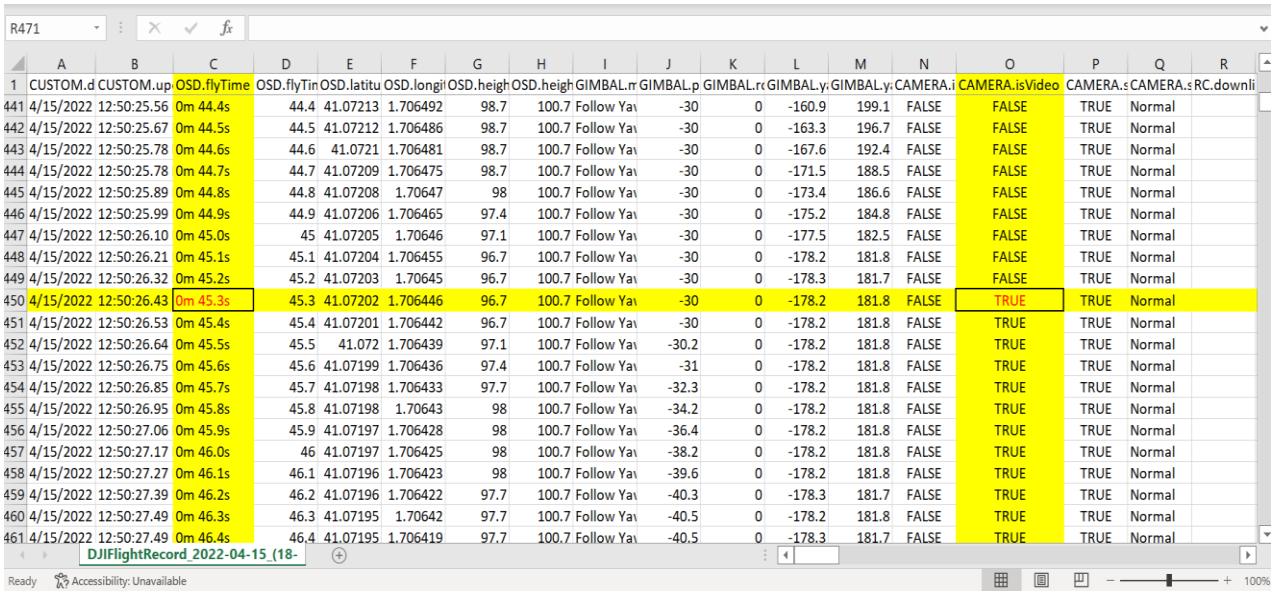

	A	B	C	D	E	F	G	H	I	J	K	L	M	N	O	P	Q	R
1	CUSTOM.d	CUSTOM.up	OSD.flyTime	OSD.flyTin	OSD.latitu	OSD.longi	OSD.heigh	OSD.heigh	GIMBAL.r	GIMBAL.p	GIMBAL.r	GIMBAL.y	GIMBAL.y	CAMERA.i	CAMERA.isVideo	CAMERA.s	CAMERA.s	RC.downli
441	4/15/2022	12:50:25.56	0m 44.4s	44.4	41.07213	1.706492	98.7	100.7	Follow Ya	-30	0	-160.9	199.1	FALSE	FALSE	TRUE	Normal	
442	4/15/2022	12:50:25.67	0m 44.5s	44.5	41.07212	1.706486	98.7	100.7	Follow Ya	-30	0	-163.3	196.7	FALSE	FALSE	TRUE	Normal	
443	4/15/2022	12:50:25.78	0m 44.6s	44.6	41.0721	1.706481	98.7	100.7	Follow Ya	-30	0	-167.6	192.4	FALSE	FALSE	TRUE	Normal	
444	4/15/2022	12:50:25.78	0m 44.7s	44.7	41.07209	1.706475	98.7	100.7	Follow Ya	-30	0	-171.5	188.5	FALSE	FALSE	TRUE	Normal	
445	4/15/2022	12:50:25.89	0m 44.8s	44.8	41.07208	1.70647	98	100.7	Follow Ya	-30	0	-173.4	186.6	FALSE	FALSE	TRUE	Normal	
446	4/15/2022	12:50:25.99	0m 44.9s	44.9	41.07206	1.706465	97.4	100.7	Follow Ya	-30	0	-175.2	184.8	FALSE	FALSE	TRUE	Normal	
447	4/15/2022	12:50:26.10	0m 45.0s	45	41.07205	1.70646	97.1	100.7	Follow Ya	-30	0	-177.5	182.5	FALSE	FALSE	TRUE	Normal	
448	4/15/2022	12:50:26.21	0m 45.1s	45.1	41.07204	1.706455	96.7	100.7	Follow Ya	-30	0	-178.2	181.8	FALSE	FALSE	TRUE	Normal	
449	4/15/2022	12:50:26.32	0m 45.2s	45.2	41.07203	1.70645	96.7	100.7	Follow Ya	-30	0	-178.3	181.7	FALSE	FALSE	TRUE	Normal	
450	4/15/2022	12:50:26.43	0m 45.3s	45.3	41.07202	1.706446	96.7	100.7	Follow Ya	-30	0	-178.2	181.8	FALSE	TRUE	TRUE	Normal	
451	4/15/2022	12:50:26.53	0m 45.4s	45.4	41.07201	1.706442	96.7	100.7	Follow Ya	-30	0	-178.2	181.8	FALSE	TRUE	TRUE	Normal	
452	4/15/2022	12:50:26.64	0m 45.5s	45.5	41.072	1.706439	97.1	100.7	Follow Ya	-30.2	0	-178.2	181.8	FALSE	TRUE	TRUE	Normal	
453	4/15/2022	12:50:26.75	0m 45.6s	45.6	41.07199	1.706436	97.4	100.7	Follow Ya	-31	0	-178.2	181.8	FALSE	TRUE	TRUE	Normal	
454	4/15/2022	12:50:26.85	0m 45.7s	45.7	41.07198	1.706433	97.7	100.7	Follow Ya	-32.3	0	-178.2	181.8	FALSE	TRUE	TRUE	Normal	
455	4/15/2022	12:50:26.95	0m 45.8s	45.8	41.07198	1.70643	98	100.7	Follow Ya	-34.2	0	-178.2	181.8	FALSE	TRUE	TRUE	Normal	
456	4/15/2022	12:50:27.06	0m 45.9s	45.9	41.07197	1.706428	98	100.7	Follow Ya	-36.4	0	-178.2	181.8	FALSE	TRUE	TRUE	Normal	
457	4/15/2022	12:50:27.17	0m 46.0s	46	41.07197	1.706425	98	100.7	Follow Ya	-38.2	0	-178.2	181.8	FALSE	TRUE	TRUE	Normal	
458	4/15/2022	12:50:27.27	0m 46.1s	46.1	41.07196	1.706423	98	100.7	Follow Ya	-39.6	0	-178.2	181.8	FALSE	TRUE	TRUE	Normal	
459	4/15/2022	12:50:27.39	0m 46.2s	46.2	41.07196	1.706422	97.7	100.7	Follow Ya	-40.3	0	-178.3	181.7	FALSE	TRUE	TRUE	Normal	
460	4/15/2022	12:50:27.49	0m 46.3s	46.3	41.07195	1.70642	97.7	100.7	Follow Ya	-40.5	0	-178.2	181.8	FALSE	TRUE	TRUE	Normal	
461	4/15/2022	12:50:27.49	0m 46.4s	46.4	41.07195	1.706419	97.7	100.7	Follow Ya	-40.5	0	-178.3	181.7	FALSE	TRUE	TRUE	Normal	

Figure 3.3- example of a Flight record csv. file for matching the video recordings ("CAMERA.isVideo") with the corresponding flight time ("OSD.flyTime") in Excel.

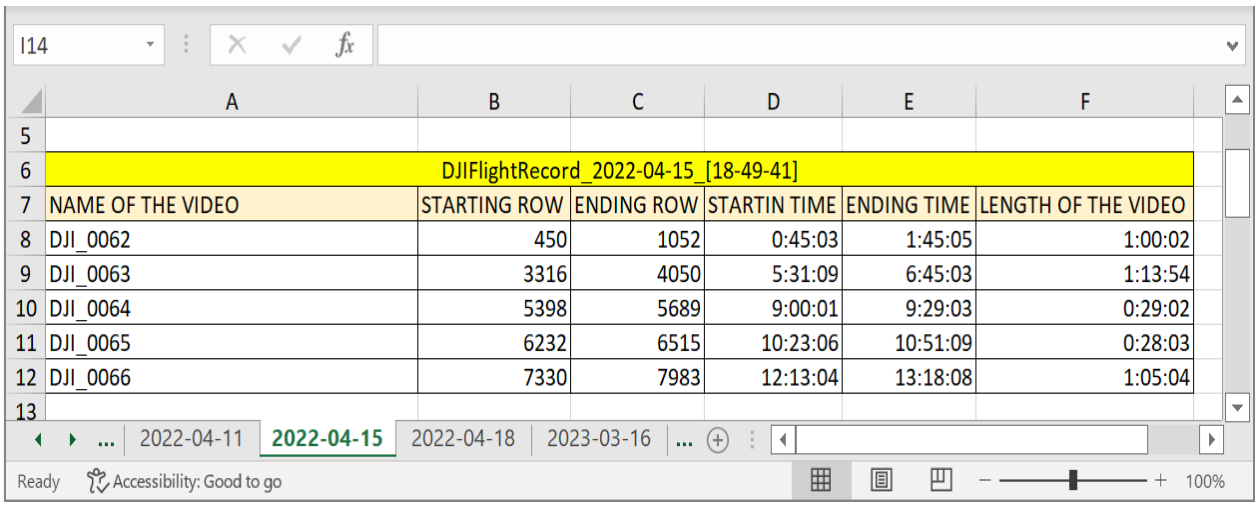

	A	B	C	D	E	F
5						
6	DJIFlightRecord_2022-04-15_[18-49-41]					
7	NAME OF THE VIDEO	STARTING ROW	ENDING ROW	STARTIN TIME	ENDING TIME	LENGTH OF THE VIDEO
8	DJI_0062	450	1052	0:45:03	1:45:05	1:00:02
9	DJI_0063	3316	4050	5:31:09	6:45:03	1:13:54
10	DJI_0064	5398	5689	9:00:01	9:29:03	0:29:02
11	DJI_0065	6232	6515	10:23:06	10:51:09	0:28:03
12	DJI_0066	7330	7983	12:13:04	13:18:08	1:05:04
13						

Figure 3.4- example of the "matched_drone_recods" excel file depicting the collected data from a Flight record csv. file to obtain the length of each video to be able to match it with real footage ("NAME OF THE VIDEO")

The drone footage was then opened and viewed with VLC Media Player (version 3.0.18). Pictures of "sample points" when the whale breaks through the surface to breath (breathing event) (Hartman *et al.*, 2020) or when the animal is close to surfacing while keeping the body in a straight vertical line (Figure 3.5) (Cheney *et al.*, 2022) were extracted in full-resolution frames with the snapshot function in the VLC Media Player (Soledade Lemos *et al.*, 2020) and were named in the following manner: name of the video, then number of the picture taken from the video, followed by the time of the snapshot (minute-second-millisecond) and the date. For

example, DJI_0928-1_00-23-8_2023-05-17.png. From individual whales the goal was to extract at least 3 images per flight, to average the future measurements in order to minimize precision errors (Durban *et. al*., 2021). However, it was not always possible due to non-ideal conditions, including environmental factors such as glare, splash, and turbidity which can blur the outline of the animal (Cheney *et al*., 2022). Furthermore, the body position of the whale is crucial as if it is not straight but arched or curved it reduces the accuracy of the measurement to a great extent (Castrillon & Bengston Nash, 2020). Afterwards, when the pictures were obtained, they went under a second assessment and were put into groups, either into "good" or to "bad" based on their quality, to get the best estimates and to further minimize the errors (Dawson *et al*., 2017; Soledade *et al*., 2022. "Bad" quality pictures (which were not in focus, or the animal was bent vertically or if the body was masked by weather conditions more than 25%) got rejected from further analysis (Soledade Lemos *et al*., 2020).

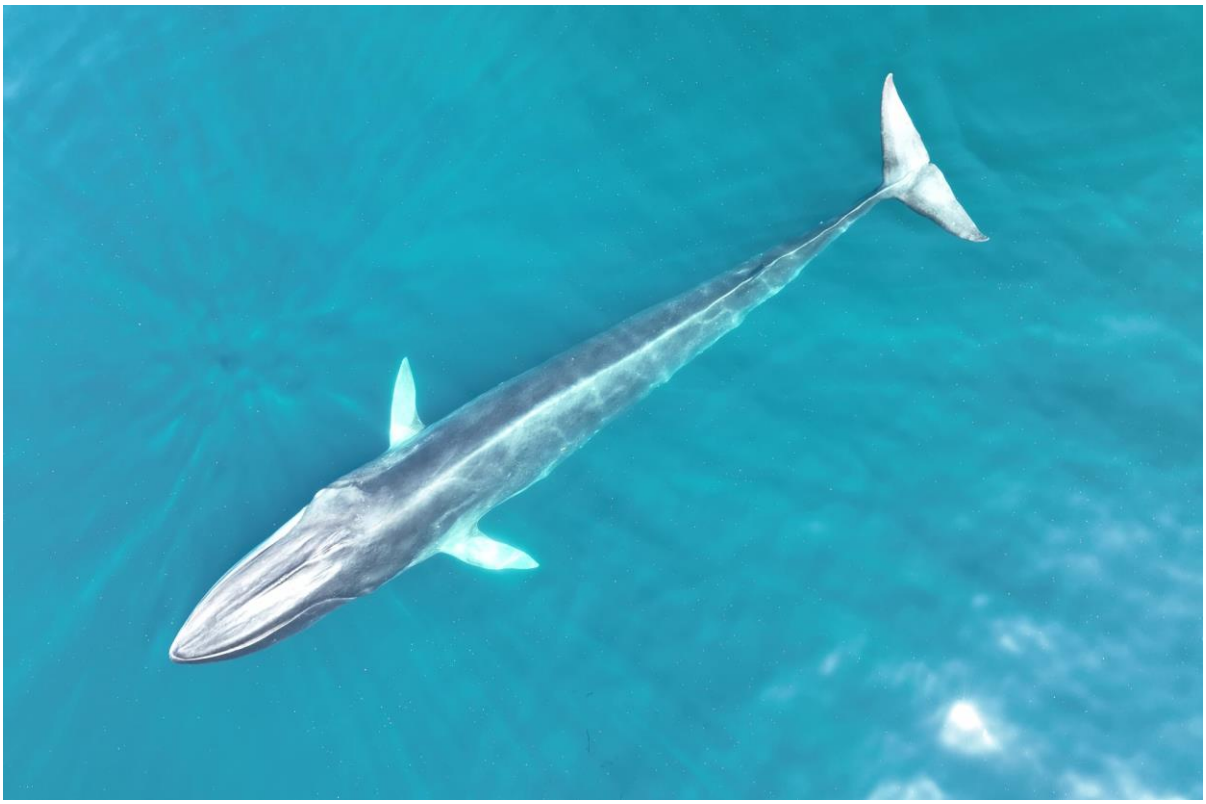

Figure 3.5- Example of the "sample point" with the desired whale position and conditions to obtain still images from drone video footage for the morphometric measurements (video taken by Eduard Degollada, 2022)

As the next step the "good" quality pictures were matched with the altitude of the drone in that specific moment when the still image was taken, by checking the beginning of the recording in

the “matched_drone_records” excel file and then opening the corresponding flight record csv. file and search in the “OSD.flyTime” column by adding the time when the picture was taken to the start time of the video and reading the height from the “OSD.height” column in the same row (Figure 3.6).

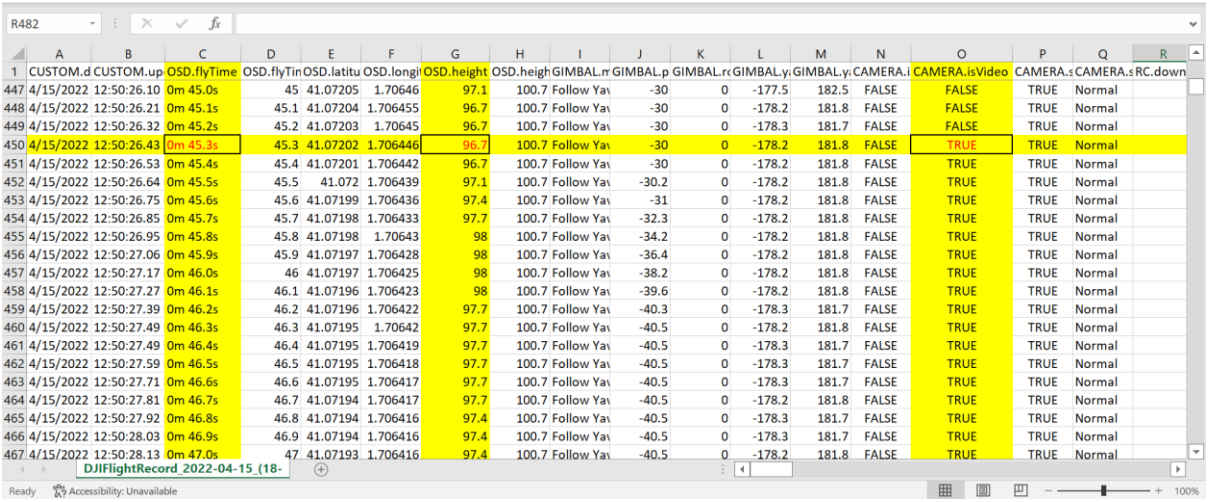

	A	B	C	D	E	F	G	H	I	J	K	L	M	N	O	P	Q	R
1	CUSTOM.d	CUSTOM.up	OSD.flyTime	OSD.flyTin	OSD.latitu	OSD.longit	OSD.height	OSD.heigh	GIMBAL.m	GIMBAL.p	GIMBAL.r	GIMBAL.y	GIMBAL.y	CAMERA.i	CAMERA.isVideo	CAMERA.s	CAMERA.s	RC.down
447	4/15/2022	12:50:26.10	0m 45.0s	45	41.07205	1.70646	97.1	100.7	Follow Yaw	-30	0	-177.5	182.5	FALSE	FALSE	TRUE	Normal	
448	4/15/2022	12:50:26.21	0m 45.1s	45.1	41.07204	1.706455	96.7	100.7	Follow Yaw	-30	0	-178.2	181.8	FALSE	FALSE	TRUE	Normal	
449	4/15/2022	12:50:26.32	0m 45.2s	45.2	41.07203	1.70645	96.7	100.7	Follow Yaw	-30	0	-178.3	181.7	FALSE	FALSE	TRUE	Normal	
450	4/15/2022	12:50:26.43	0m 45.3s	45.3	41.07202	1.706446	96.7	100.7	Follow Yaw	-30	0	-178.2	181.8	FALSE	TRUE	TRUE	Normal	
451	4/15/2022	12:50:26.53	0m 45.4s	45.4	41.07201	1.706442	96.7	100.7	Follow Yaw	-30	0	-178.2	181.8	FALSE	TRUE	TRUE	Normal	
452	4/15/2022	12:50:26.64	0m 45.5s	45.5	41.072	1.706439	97.1	100.7	Follow Yaw	-30.2	0	-178.2	181.8	FALSE	TRUE	TRUE	Normal	
453	4/15/2022	12:50:26.75	0m 45.6s	45.6	41.07199	1.706436	97.4	100.7	Follow Yaw	-31	0	-178.2	181.8	FALSE	TRUE	TRUE	Normal	
454	4/15/2022	12:50:26.85	0m 45.7s	45.7	41.07198	1.706433	97.7	100.7	Follow Yaw	-32.3	0	-178.2	181.8	FALSE	TRUE	TRUE	Normal	
455	4/15/2022	12:50:26.95	0m 45.8s	45.8	41.07198	1.70643	98	100.7	Follow Yaw	-34.2	0	-178.2	181.8	FALSE	TRUE	TRUE	Normal	
456	4/15/2022	12:50:27.06	0m 45.9s	45.9	41.07197	1.706428	98	100.7	Follow Yaw	-36.4	0	-178.2	181.8	FALSE	TRUE	TRUE	Normal	
457	4/15/2022	12:50:27.17	0m 46.0s	46	41.07197	1.706425	98	100.7	Follow Yaw	-38.2	0	-178.2	181.8	FALSE	TRUE	TRUE	Normal	
458	4/15/2022	12:50:27.27	0m 46.1s	46.1	41.07196	1.706423	98	100.7	Follow Yaw	-39.6	0	-178.2	181.8	FALSE	TRUE	TRUE	Normal	
459	4/15/2022	12:50:27.39	0m 46.2s	46.2	41.07196	1.706422	97.7	100.7	Follow Yaw	-40.3	0	-178.3	181.7	FALSE	TRUE	TRUE	Normal	
460	4/15/2022	12:50:27.49	0m 46.3s	46.3	41.07195	1.70642	97.7	100.7	Follow Yaw	-40.5	0	-178.2	181.8	FALSE	TRUE	TRUE	Normal	
461	4/15/2022	12:50:27.49	0m 46.4s	46.4	41.07195	1.706419	97.7	100.7	Follow Yaw	-40.5	0	-178.3	181.7	FALSE	TRUE	TRUE	Normal	
462	4/15/2022	12:50:27.59	0m 46.5s	46.5	41.07195	1.706418	97.7	100.7	Follow Yaw	-40.5	0	-178.3	181.7	FALSE	TRUE	TRUE	Normal	
463	4/15/2022	12:50:27.71	0m 46.6s	46.6	41.07195	1.706417	97.7	100.7	Follow Yaw	-40.5	0	-178.3	181.7	FALSE	TRUE	TRUE	Normal	
464	4/15/2022	12:50:27.81	0m 46.7s	46.7	41.07194	1.706417	97.7	100.7	Follow Yaw	-40.5	0	-178.2	181.8	FALSE	TRUE	TRUE	Normal	
465	4/15/2022	12:50:27.92	0m 46.8s	46.8	41.07194	1.706416	97.4	100.7	Follow Yaw	-40.5	0	-178.3	181.7	FALSE	TRUE	TRUE	Normal	
466	4/15/2022	12:50:28.03	0m 46.9s	46.9	41.07194	1.706416	97.4	100.7	Follow Yaw	-40.5	0	-178.3	181.7	FALSE	TRUE	TRUE	Normal	
467	4/15/2022	12:50:28.13	0m 47.0s	47	41.07193	1.706416	97.4	100.7	Follow Yaw	-40.5	0	-178.2	181.8	FALSE	TRUE	TRUE	Normal	

Figure 3.6- Example of the Flight record csv. while matching the correspond height to the obtained still image

Consequently, the pictures are imported one by one into MorphoMertiX (an accessible, open-source program, built to measure accurate morphometric parameters of free ranging cetaceans) to carry out the measurements (Figure 3.7) (Torres & Bierlich, 2020). After opening the image the program requires to enter the name of the picture and to enter the following parameters of the drone; focal length (which is in case of the used Mavic 2 Pro is 28 mm and for Mavic 3 is 24 mm), the pixel dimension (sensor width / image width, which depends on the resolution of the footage, in case of 4K resolution the Mavic 2 Pro is 0.0034375 mm/pixel and for Mavic 3 is 0.0045026), altitude (of the UAS at the exact time when the picture was taken, obtained from the flight record), as well as the number of width segments to be measured (Torres & Bierlich, 2020). With these attributes personalized morphometric measurements were calculated, including standard cetacean body proportion measurements, such as the total length (TL; from the tip of the rostrum, until the notch of the fluke), fluke spread (FS), distance from the snout to blowhole (SB), distance from snout to dorsal fin (SD), distance from snout to anterior insertion of the flipper (SAF), distance from snout to posterior insertion of the flipper (SPF), anterior flipper length (AFL), the posterior flipper length (PFL), and the width between the eyes (ETE) (Figure 3.8) (Ratnaswamy & Winn, 1993). Moreover, the general width was

measured at 20 locations, by splitting the animal into 20 equal segments along the length of body (TL) (Christiansen *et al*., 2018), that were at equal distances from each other, and then at each section the two outlines were marked manually, between which the measurement was calculated (Aoki *et al*., 2021). Lipid storage does not accumulate on the head and the extremities (fins, fluke) consequently only the torso area (where the volume varies the most between 20 to 60 percent of the total body length) was used to calculate the energy reserves (Soledade Lemos *et al*., 2020). All the above-mentioned parameters were manually designated for the distance measurements (number of pixels) (Gray *et al*., 2019).

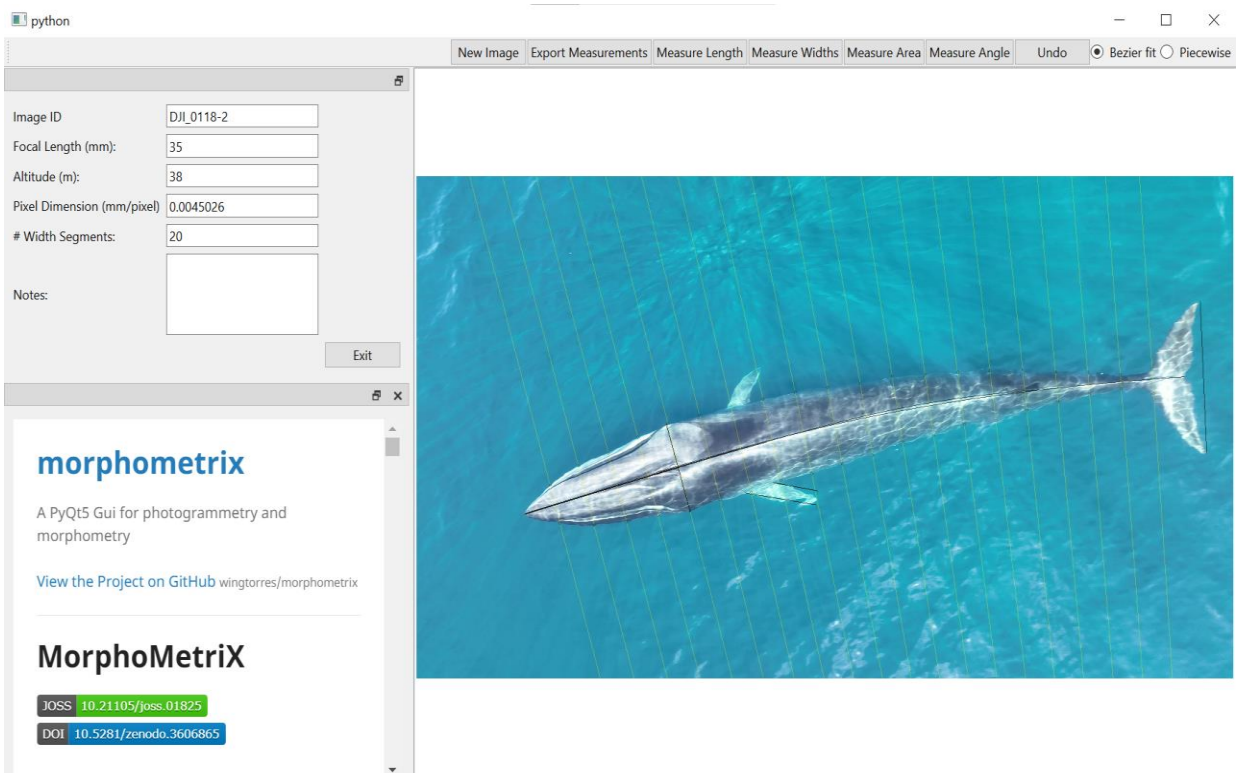

Figure 3.7- MorphoMetriX program's interface with a measured picture of the field season 2021

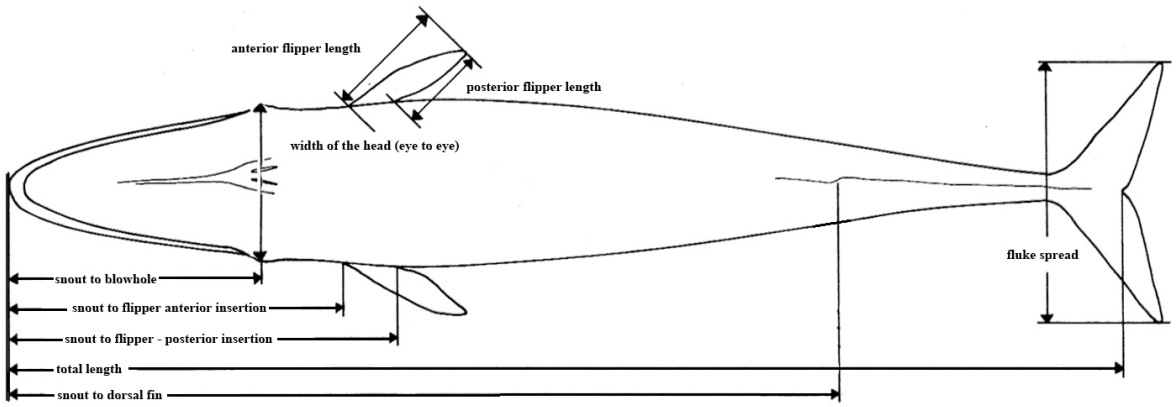

Figure 3.8- Representative drawing of a Fin whale from above with the applied morphometric and standard body proportion measurements from Ratnaswamy & Winn, 1993, with some added parameters specific for this project (edited by: Anson Aguirre Firth)

Based on the previously given drone attributes (pixel dimension, focal length, altitude) the program automatically transformed the manual pixel-based measurements into accurate distance units. Firstly, the ground sampling distance (GSD) which is the representation of individual pixel area stretched out on the ground is being calculated by dividing the altitude with the focal length and multiplying its result with the pixel dimension. Afterwards, for each manually designated length measurement is multiplied by the previously calculated GSD, which results in a real-life size measurement in meters (Figure 3.9) (Torres & Bierlic, 2020).

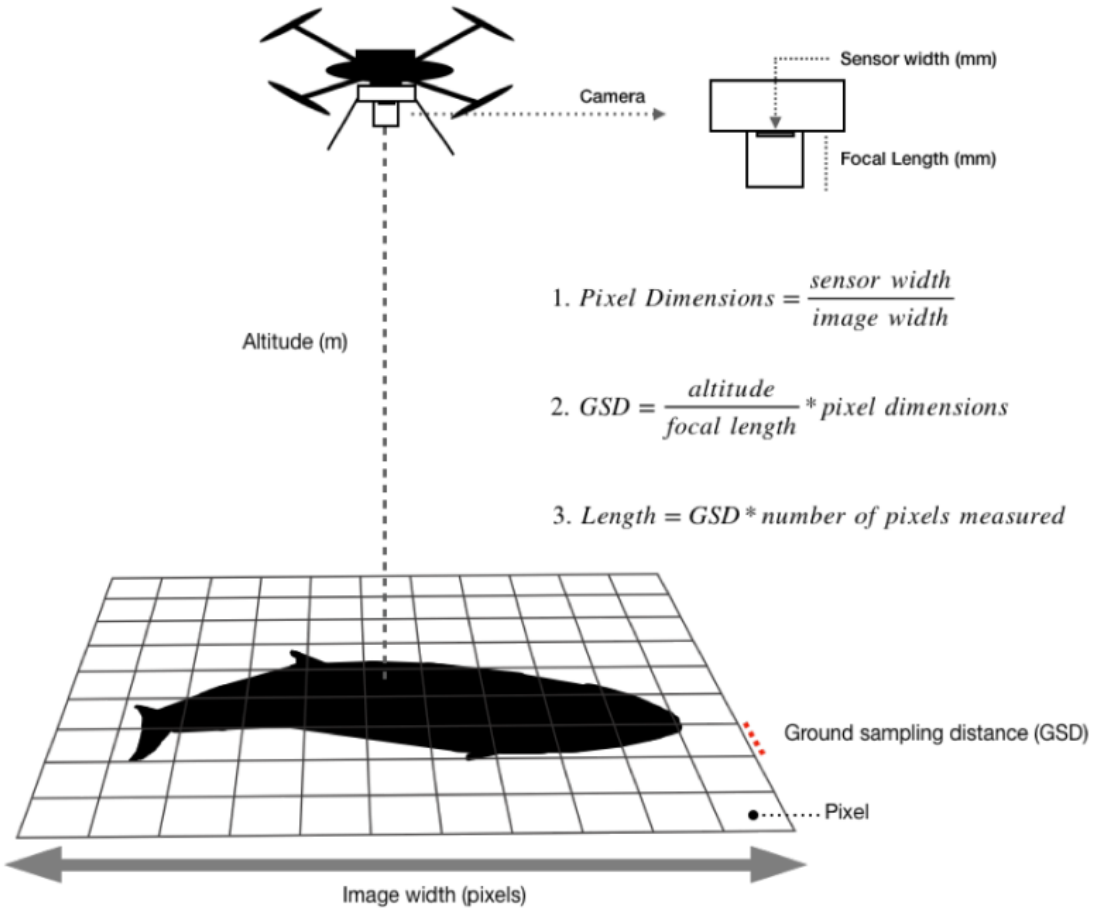

Figure 3.9- Explanation of the automatic conversion of the measurements by MorphoMetrix Torres & Bierlic, 2020

Each photogrammetric measurement in MorphoMetriX is exported as a .csv document, and besides a photograph depicting the conducted measurements.

These single .csv data files were merged together into one csv. directory by the date using the main function of the CollatriX software. Afterwards, the "whale body condition" function was run on the merged outputs to calculate the body volume (BV) based on the perpendicular width measurements across the body (Burnett *et al*., 2018) (between 20% to 60% of the total length), giving a three-dimensional measurement output in m^3.

Furthermore, the body area index (BAI) was calculated (which is a continuous, scale-invariant and unitless measure) (Soledade *et al*., 2020), to assess the relative amount of energy reserve (Hirtle at. Al., 2022). The BAI was measured with two different methods; the parabola (when the width measurements are used to create the curvature of the body shape and the surface area within is calculated) and the trapezoid (when trapezoids between the width segments are created and the surface area is calculated by summing these individual trapezoid fields)

(Christiansen *et al.*, 2018) between 20 to 60% of the total length, obtaining a continuous, unitless metric (Soledade Lemos *et al.*, 2020), by using the same function of CollatriX.
Moreover, the collated outputs including the BAI and the BV calculations were merged together per year. In which document the Drone ID and the Gender of the whales (if known) were matched and added from EDMAKTUB's ID catalog. Finally, the measurement outputs of the same individual within the same day were averaged to obtain the most accurate measurement and minimize the error raising from the manual designations (Durban *et. al*., 2021).

Additionally, another document was created where the following body proportions were calculated for each whale measurement from MorphoMetriX; 'fluke spread' to 'total length' (FS:TL), 'snout to blowhole' to 'total length' (SB:TL), 'snout to dorsal to 'total length' (SD:TL), 'snout to anterior flipper' to 'total length' (SAF:TL), 'snout to posterior flipper' to 'total length' (SPF:TL), 'eye to eye' to 'snout to blowhole' (ETE:SB), 'anterior flipper length' to 'snout to blowhole' (AFL:SB), 'posterior flipper length' to 'snout to blowhole' (PFL:SB), 'eye to eye' to 'fluke spread' (ETE:FS), 'anterior flipper spread' to 'fluke spread' (AFL:FS), 'posterior flipper length' to 'fluke spread' (PFL:FS), 'snout to anterior flipper' to 'snout to posterior flipper' (SAF:SPF), 'anterior flipper length' to 'posterior flipper length' (AFL:PFL). These values were matched to the Drone ID and the Gender of the whales (if known) were matched and added from EDMAKTUB's ID catalog. Finally, the measurement outputs of the same individual within the same day were averaged to obtain the most accurate measurement (Durban *et. al.*, 2021) and minimize the error raising from the manual designations (Dawson *et al*., 2017; Soledade *et al.*, 2020).

3.3.3 Statistical Analysis

Statistical analyses were performed in R (version 4.0.3) and RStudio (Version: 2023.03.1+446 (R Core Team, 2023)). The variables were tested for normal distribution using Shapiro-Wilk test (p-value<0.05), and Levene's test was applied to test the homogeneity (p-value<0.05). Furthermore, for each variable a boxplot was created to detect any extreme values (outliers) prior further analysis. When normality and homogeneity were not found a logarithmic

transformation was performed of all variables to reduce the effects of outliers and to obtain data closer to normal distribution.

Afterwards, to investigate the relation (correlation) between the logarithmically transformed body parameters (TL, SB, SD, SAF, SPF, AFL, PFL, FS, ETE) a correlation matrix was created, using the following package: GGally. For further visualization of the degree of relation between highly correlated variables ggplots were constructed, using the ggplot2 package. Based on the division of the samples of the two strongly correlated variables (ETE, TL) the data was divided into three groups based on the length of the animals. Therefore, the animals were assigned into the following groups: „SMALL" including animals under 14 meters, „MEDIUM" animals between 14 and 19 and „LARGE" which includes whales above 20-meter length.

To identify the significance of the relationship between highly correlated body parameters (variables) Linear Models were obtained. All of which models were inspected according to linear models' assumptions beforehand, of normality and homogeneity of residuals and related diagnostic plots were performed. The models which attained an adjusted R-square close to 1, had significant variables, and had residuals that were adequate, were accepted. These body parameters went under further analysis to determine if any factors such as gender or size has an influence on their relation. This effect was determined by creating new Linear Models of the same body parts and adding a factor into the model. When significant influence of the tested factors (gender, size) were observed separated Linear Models were created for each subgroup (female, male or each size group) to identify the precise differences among them. Models obtaining significant results were plotted together, showcasing the separated models per group, scaled to the original dataset, using the following packages: ggplot2, GGally, hrbrthemes.

The difference between the means of the two BAI measurement methods (trapezoid and parabola) were examined by running a non-parametric (independent) two-samples Wilcoxon test ($p\text{-value}<0.05$). Moreover, Kruskal-Wallis test ($p\text{-value}<0.05$) was applied to test for potential significant differences existing between the BAI measurements among genders and size groups, for each methods. Additionally, a Kruskal-Wallis test ($p\text{-value}<0.05$) was also used to investigate differences between the obtained BV values from the three examined seasons.

4. Results

For this study a total of 366 aerial footage (2021: 193, 2022: 109, 2023: 67) were analyzed, from which 1099 still images (2021: 426, 2022: 256, 2023: 415) were captured and measured, depicting 82 individual fin whales in total.
Further, two videos and 20 pictures of the calibration object were used to measure the uncertainty from altitude measurements (Best & Ruther, 1992; Dawson *et al*., 2017; Soledade *et al*., 2020; Torres & Bierlich, 2020).

4.1 Uncertainties from altitude measurements

The "absolute error" was calculated by obtaining the differences between the outputs of the calibration object measurements and the real size of the calibration object and by taking the mean of the absolute value of the results. For the Mavic Pro 2 the average absolute error is: 0,36 and in the case of Mavic 3 the absolute error is: 0,41. Afterwards, the "average photogrammetric error" was determined by dividing the "absolute error" with the real size of the calibration object (average photogrammetric error for Mavic Pro 2: 0,025175 (2,5%) and for the Mavic 3 it is 0,098561 (9,8%) (Ratnaswamy & Winn, 1993).

4.2 Whale body measurements

Fin whales in the Garraf coast during the time period of 2021-2023 had the average body length of 16.75 meters, with the smallest measured animal being a 9.49 meters long calf and the largest a 24.45 meters long female. The average body length throughout the three seasons of females were 18.08 meters and males were 16.63 meters, with the average difference of 1.98 meters.

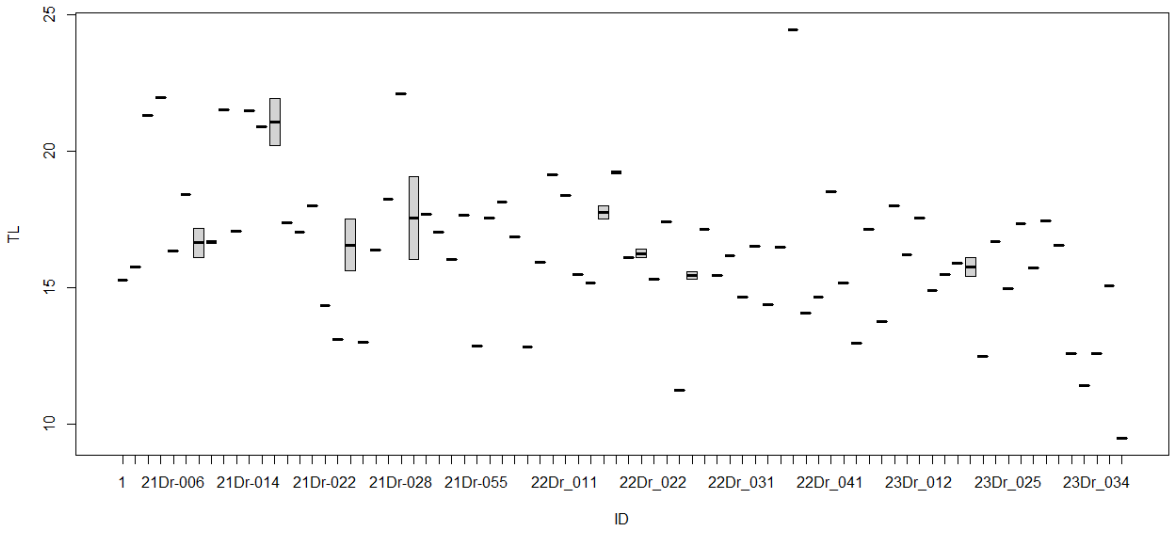

Figure 4.1- Deviation of total length measurements based on the animals ID over the three examined seasons

Figure 4.1 depicts the deviation of the total length measurements throughout 2021 till 2023, by individual animals. The majority show no or minimal deviation, and some animals have moderate deviation. This inconsistency arises from higher number of performed measurements of the same animal over the three seasons. Thereby, the outputs of the measurements proved to be reliable for further analysis.

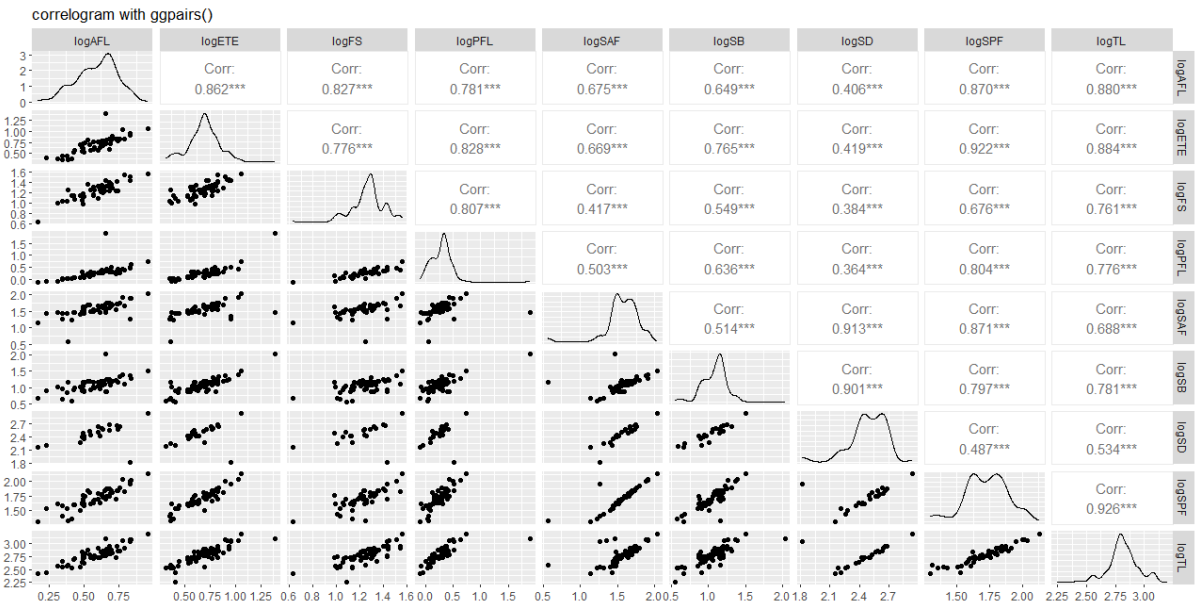

Figure 4.2- correlation matrix of logarithmically transformed standard cetacean body measurements (TL, FS, SB, SD, SAF, SPF, AFL, PFL, ETE)

Figure 4.2 showcases the correlation amongst the values of standard cetacean body measurements described by Ratnaswamy & Winn in 1993 (logarithmically transformed). Each attribute correlates between 0,364 (moderate correlation) and 0,926 (very strong correlation), where the attributes having the lowest correlation coefficient are the snout to dorsal fin (SD) and the posterior flipper length (PFL). While the strongest correlation appears to be between the total length (TL) and the snout to posterior flipper (SPF). Furthermore, there is very strong correlation between the eye-to-eye width (ETE) and snout to posterior flipper (SPF), also between the snout to dorsal fin (SD) and the snout to anterior flipper (SAF). Based on the linearity of the scatter plot the snout to anterior flipper (SAF) and the snout to posterior flipper (SPF), which attributes provide the width of the flipper, has a very strong relationship (Figure 4.3).

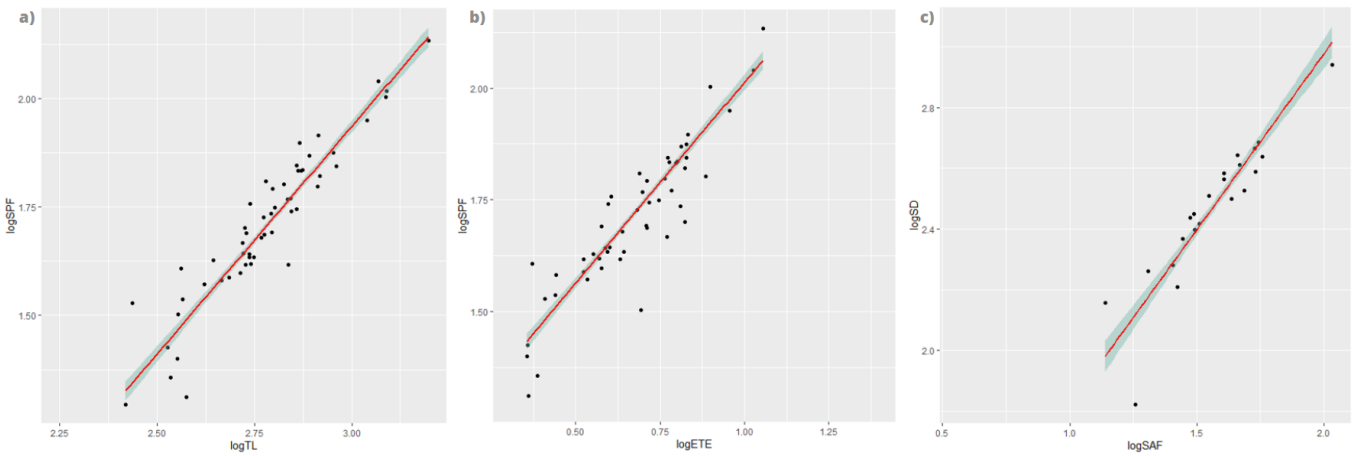

Figure 4.3- ggplots, on graph a; logTL(x axis) and logSPF(y axis), on graph b; logETE (x axis) in relation with logSPF (y axis) and on graph c; a ggplot of logSAF (x axis) and logSD (y axis)

The graphs above (Figure 4.3) depicting the relationship between the body parameters with the strongest correlation coefficient, in descending order. The first plot (Figure 4.3.a) visualizes the total length in relation to the snout to posterior flipper length, the second (Figure 4.3.b) showcases the eye-to-eye distance in relation to the snout to posterior flipper, and the last graph (Figure 4.3.c), the snout to anterior flipper length to the snout to dorsal fin distance. All of which obtained a substantial, increasing tendency, indicating the parameters positive relation.

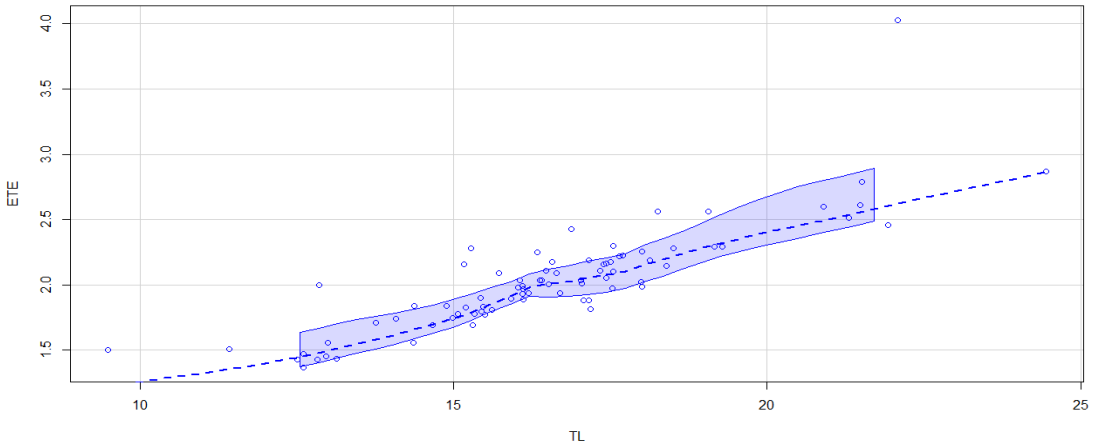

Figure 4.4- scatter plot of the relationship of the following measurements; total length (TL(logarithmically transformed)) and eye-to-eye distance (ETE(logarithmically transformed)). X axis is the TL (logarithmically transformation) in meters and the y axis is the ETE(logarithmically transformation) in meters.

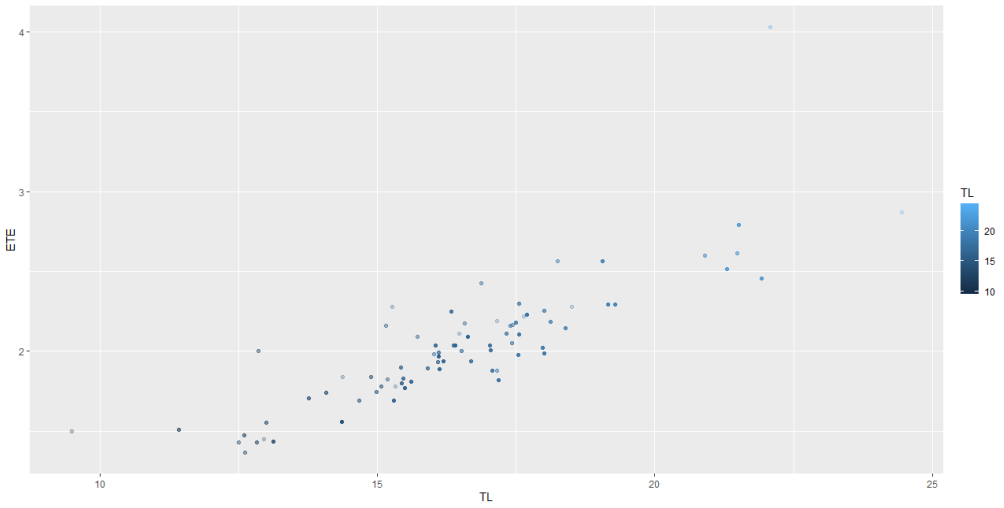

Figure 4.5 Scatter plot representing the relation between the TL and the ETE. The x axis is the TL (logarithmically transformation) in meters and the y axis is the ETE(logarithmically transformation) in meters.

Figure 4.4 depicts the positive relationship between the two variables (TL, ETE) due to the positive slope, representing the linked increase of the eye-to-eye distance, simultaneously with the increasing body length. The scatter plot also illustrates that the slope shall be divided into separated trends as whales of different body length obtain different tendencies. Furthermore, based on Figure 4.5, there are three accumulations of dots (which represents individual animals), dividing the data into three groups based on size. Therefore, the animals were

assigned into three size groups: „SMALL" including animals under 14 meters, „MEDIUM" animals between 14 and 19 and „LARGE" which includes whales above 20-meter length.

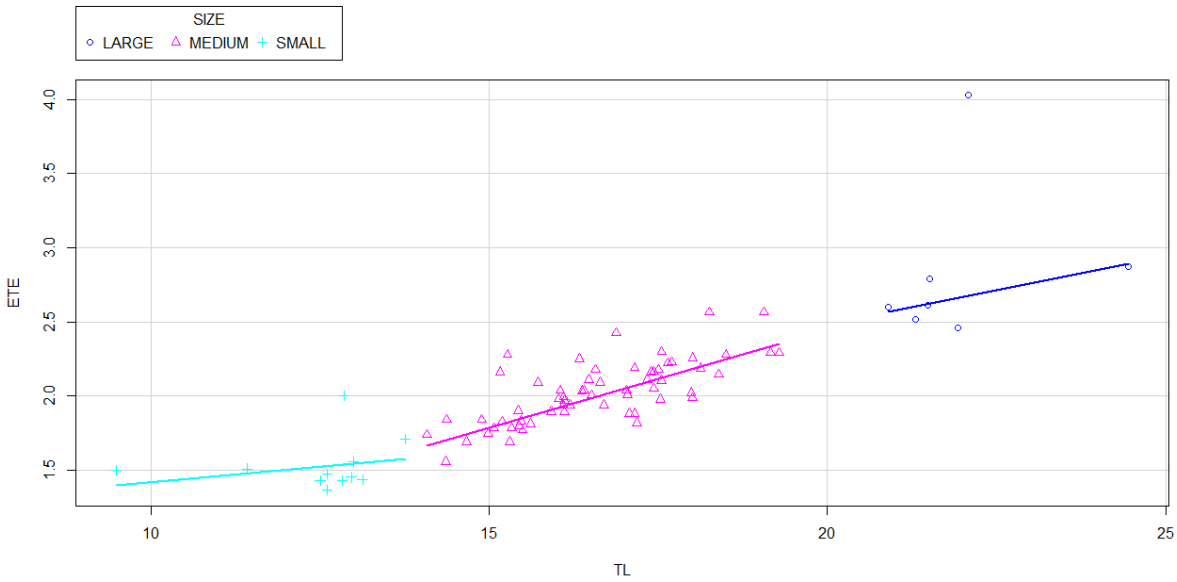

Figure 4.6 Scatter plot of the relationship between the total length (x axis) and eye-to-eye (y axis) of the newly created size group, with the different trend lines.

The affinity between TL and ETE differs among size groups as presented on figure 4.6, each of these classes obtain distinctive positive tendencies. All of which are a steady, moderately increasing slopes, however the size group "SMALL" attain the least significant increase, followed by the "LARGE" group with a considerably steeper slope and the most significant belongs to the "MEDIUM" size group.

4.2.1 Relation between the ETE and the TL

To assess the relation within the eye-to-eye distance and the total body length furthermore, to compare this amongst genders a linear model of the logarithmically transformed variables ETE and TL grouped by genders was created following the equation of; ETE = exp(-2.50 + 1.13 TL + Gender). The model had an adjusted R square of 0.8843, and each variable showed high degree of significance (<0.001), moreover the distribution of residuals validated the model, thereby it was accepted (See Figures 8.1 and 8.2 in the Annex). Afterwards, separated linear models were created based on gender; for the females the following: ETE = exp(-2.21 + 1.03 TL), this model obtained the adjusted R square of 0.8513 and both variables showed high

degree of significance (<0.001), the residuals validated the model, therefore it was accepted (see Figure 8.3, 8.4 in the Annex). And the males: ETE = exp(-3.16 + 1.38 TL), this model obtained the adjusted R square of 0.9661 and both variables showed high degree of significance (<0.001), residuals validated the model, therefore it was accepted (see Figure 8.5, 8.6 in the Annex).

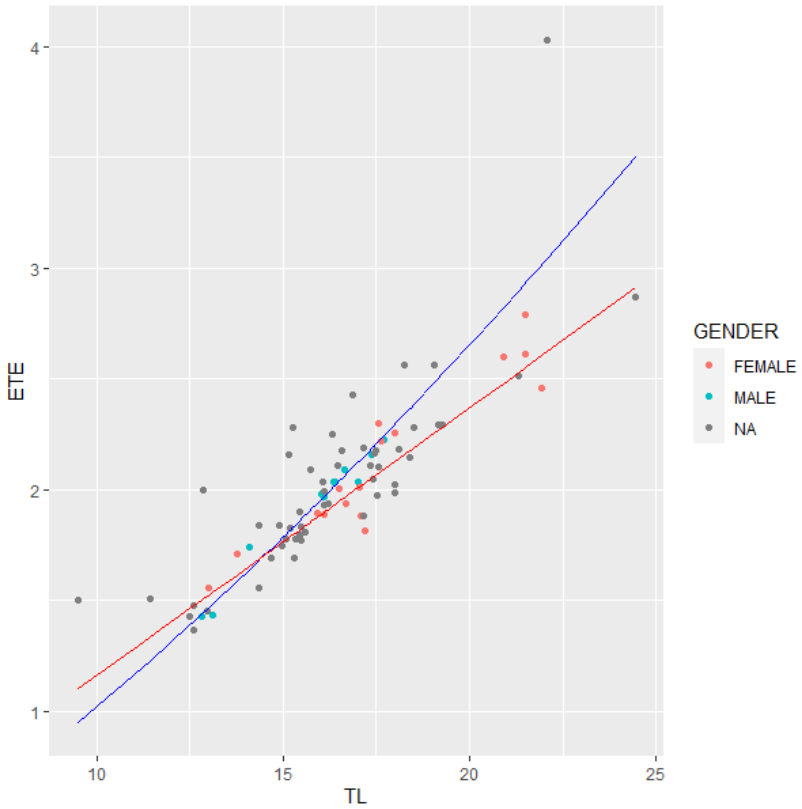

Figure 4.7- Scatterplot of the Linear regression models compairing the logarithmically transformed eye to eye distance to the logarithmically transformed total length by both genders, scaled to the original dataset ; total length (TL as the x axis) and eye to eye distance (ETE as the y axis)

The figure above (Figure 4.7) depicts the results of the previouse linear models, showcasing the relation between the total length of the animals to the eye-to-eye distance for both genders. For this model and plot 28 animals with known gender (9 males, and 17 females) were used. As the sample size was higher of females, withal there were more variablity within, which was

also seen in the linear model as well (Figure 8.3, 8.4 in the Annex), which accuracy was lower than the model's of the male individuals (Figure 8.5, 8.6 in the Annex).

Both genders obtained positively increasing tendencies, however males had a steeper upward trajectory. The two slopes cross at the close viccinity of 14.5 meters length, at this body size the proportion of these two attributes (ETE, TL) swap between genders, and starts to deviate more from each other. Under this point, in this size range males have smaller ETE distance than females, which changes to the oposite above 15 meters total length.

However, to obtain a more reliable result a higher sample size is necessary.

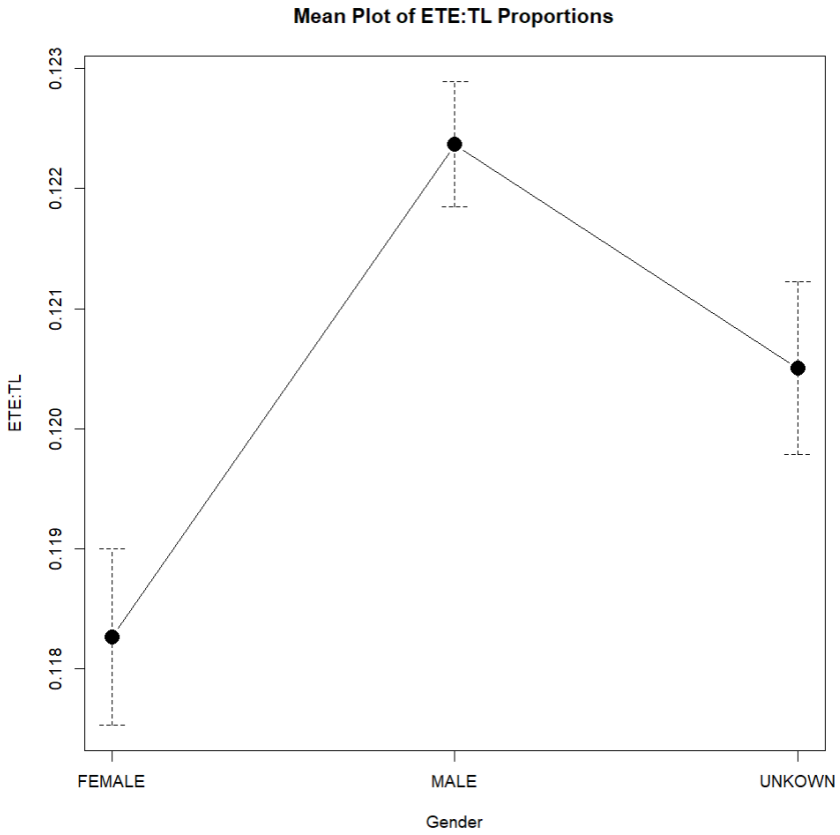

Figure 4.8- Plot of the means of the proportions of eye-to-eye distance to the total length, ETE:TL

The mean plot on Figure 4.8, represents a significant difference of the proportion of the ETE distance compared to the total length between the two genders, where males obtained a considerably larger proportion of the ETE over the females. While the group with unknown sex lies between these two extremes as it is a mix of both.

4.2.2 Relation between AFL and the TL

To clarify the relation between the following variables: logarithmically transformed AFL and TL a linear model was created by the group sizes and compare the growth trend of these body parts. The result is the following; AFL = exp(-2.31 + 1.01 TL + SIZE GROUPS), obtaining 0.7805 adjusted R square, with four significant variables out of the which two were at the significance level of <0.001 including the intercept and the logarithmically transformed TL, while the remaining two ("SMALL" and "MEDIUM" size groups) were at the significance level of <0.01 (Figure 8.7 in the Annex). The distribution of the residuals validated the model therefore it was accepted (Figure 8.8 in the Annex).

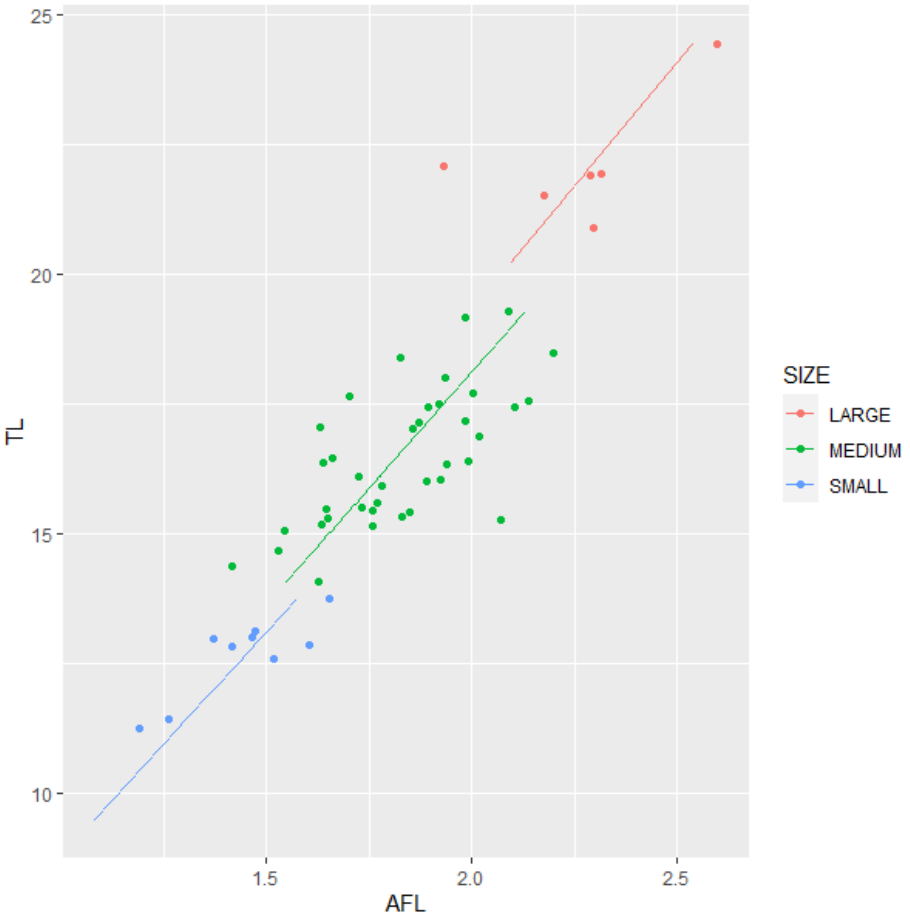

Figure 4.9- Scatterplot of the linear regression models compairing the anterior flipper length to the total length by size groups, scaled to the original dataset ; logaritmically transformed anterior flipper length (AFL as the x axis) and logaritmically transformed total length (TL as the y axis)

The plot on Figure 4.9, presents the linear regressions of the previous linear models of the logarithmically transformed TL and AFL based on the size, where each line represents a certain size class. All the three size groups have similar slopes however, the initial points are different, as there is a jump/space between them, due to the difference of the mean body length of the groups.

Due to missing values the model only contains fifty-three individual whales, from which 9 small, 38 medium and 6 large animals. However, to obtain a more reliable result a higher sample size is necessary.

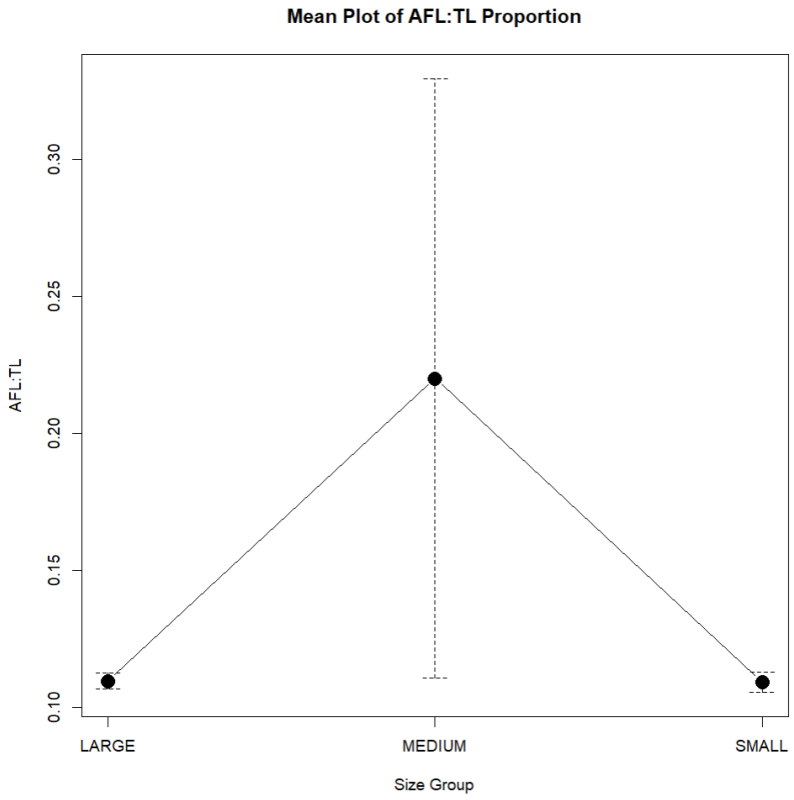

Figure 4.10- Plot of the means of the proportions of anterior flipper length to the total length, AFL:TL

The plot representing the means of the AFL:TL proportions among the three size groups. The size of the anterior flipper length proportionally the same compared to the total length in the "SMALL" and in the "LARGE" size groups. In comparison, in the "MEDIUM" size group has a proportionally bigger flipper size compared to the total length, However, this group also has much more deviation.

4.2.3 Relation between AFL and FS

To assess the relation between the anterior flipper length and the fluke spread within different sized animals the following linear model was created by the following equation: AFL = exp(0.045 + 0.54 FS + Size groups). This model obtained an Adjusted R-square of 0.8164, and all three variables has a high degree of significant (<0.001), furthermore the residuals validated the model (Figure 8.9, 8.10 in Annex). Afterwards, the tendencies of the model for each size group were visualized scaled to the original measurements of the dataset on a scatterplot (Figure 4.11).

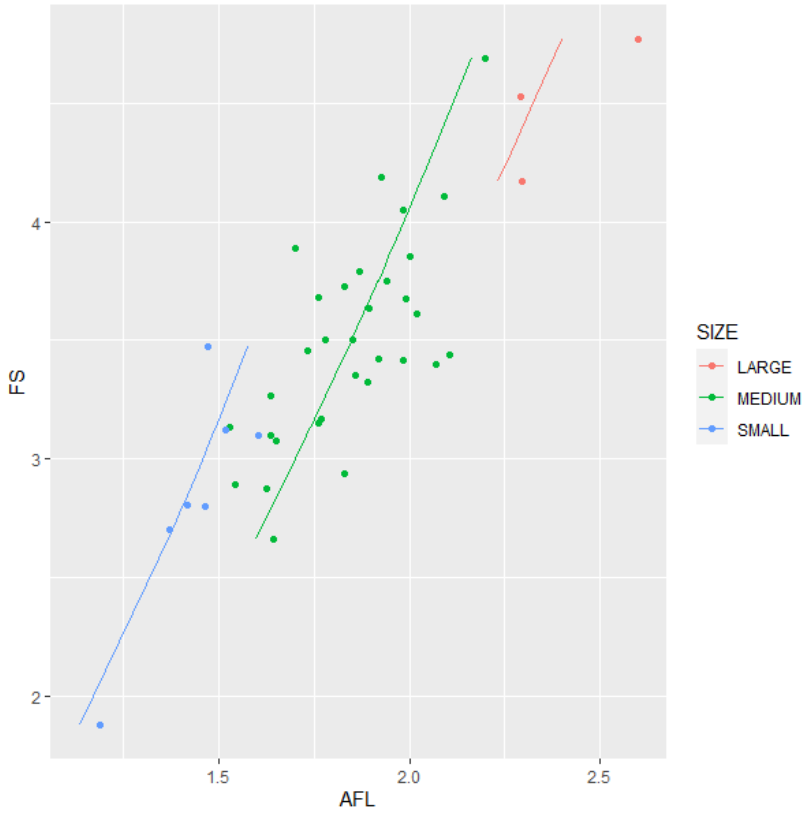

Figure 4.11- Scatterplot of the linear regression models compairing the logarithmically transformed anterior flipper length to the logarithmically transformed fluke spread by size groups, scaled to the original dataset ; anterior flipper length (AFL as the x axis) and fluke spread distance (FS as the y axis)

The plot on Figure 4.11, displays the relationship of the (logarithmically transformed) anterior flipper length and the (logarithmically transformed) fluke spread for each size groups, based on the previously mentioned linear models. Similar tendencies were obtained by all classes,

with substantial increase, visible on the steep, positive slopes. The most dramatic increase was attained by the “SMALL” size group, followed close by the other two groups (“MEDIUM”, “LARGE”) which had very similar slopes.

Due to missing values the model only contains forty-two individual whales, from which 7 small, 32 medium and 3 large animals. However, to obtain a more representative result a higher sample size is necessary.

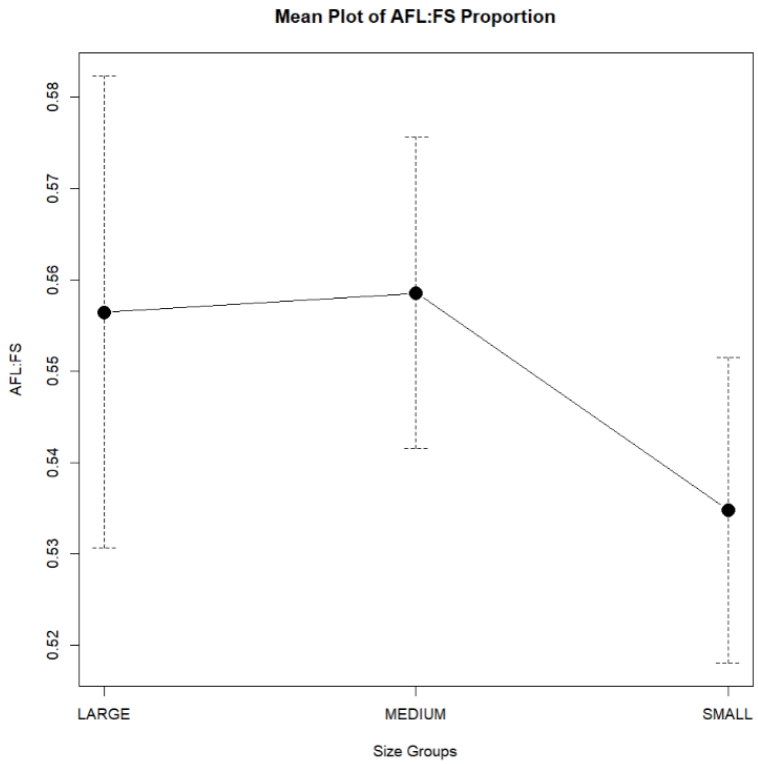

Figure 4.12 Plot of the means of the proportions of anterior flipper length (AFL) to the fluke spread (FS), AFL:FS

The plot visible on Figure 4.12, shows that proportion of the AFL to the FS is smaller within the group small, while in the large group the AFL proportion is higher compared to the FS, withal this size groups also obtains the highest deviation.

4.2.4 Growth rates of recaptured individuals

The following graphs in Figure 4.13, presents three individual fin whales that were recaptured between the studied three foraging seasons. On the graph a) from Figure 4.13, the individual 21Dr-017's growth is represented. This animal is a confirmed female that was first sighted in 2021 and recaptured in 2023. Between this time interval the whale grew 1.77 meters.

The second graph on Figure 4.13.b is about the individual 21Dr-024 with unknown gender. This whale grew 1.9 meters in two years. And the final graph (Figure 4.13.c) shows the growth of the individual 21Dr-029 (unknown gender), which animal's body length increased with exactly 3 meters over two years.

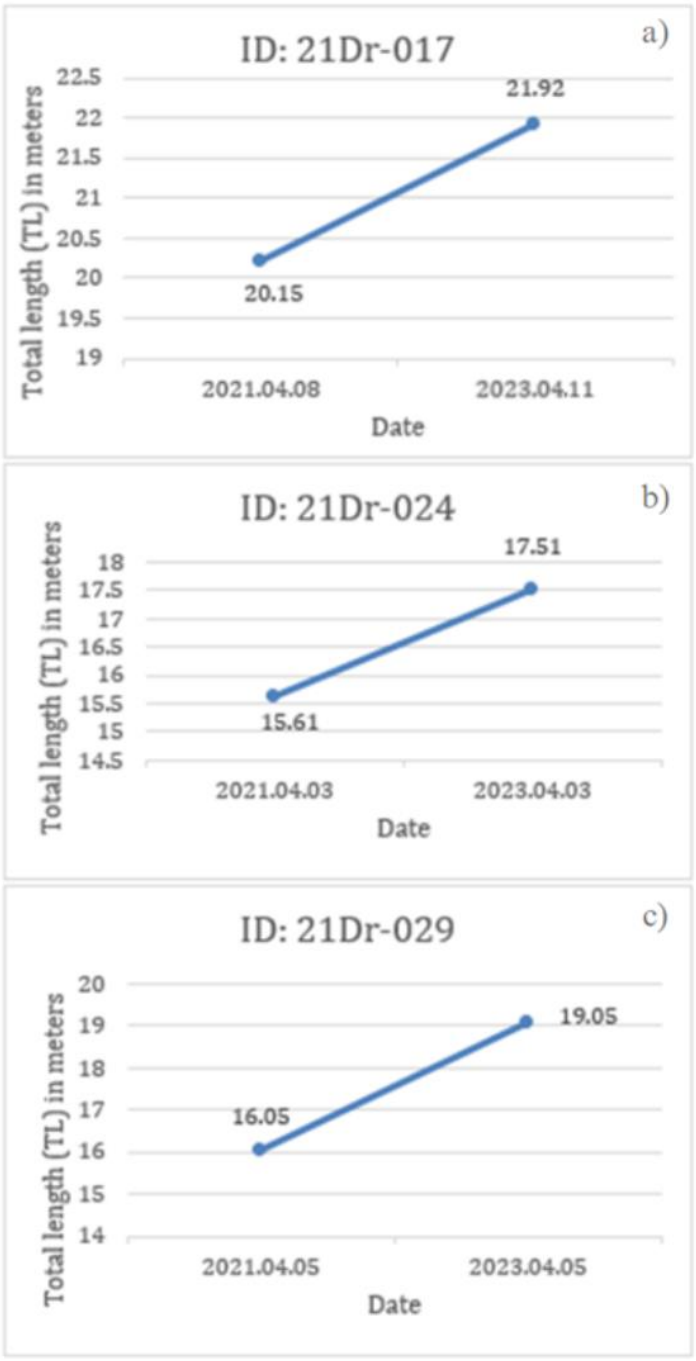

Figure 4.13- Growth of three recaptured animals between recapture dates. The graphs represent the following identified whales; on figure 4.13.a 21Dr-017, on figure 4.13.b 21Dr-024 and on figure 4.13.c 21Dr-029.

4.2.5 BAI evolution

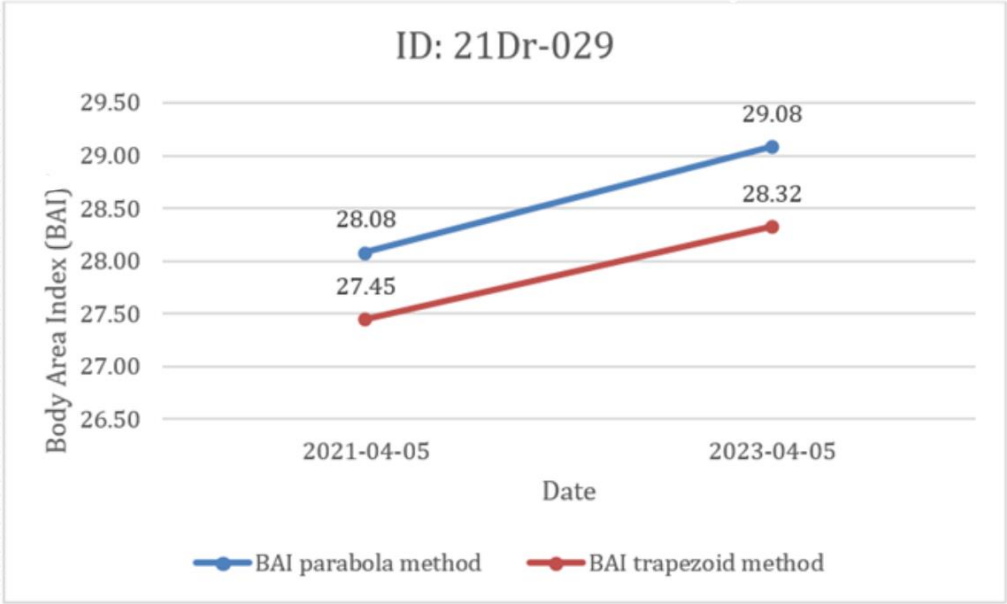

Figure 4.14- Graph of the BAI evolution of the individual 21Dr-029 between two years

The whale 21Dr-029 had a slight increase in its BAI from 2021 to 2023 which is seen on Figure 4.14, The BAI increased with approximately one order of magnitude based on the output of both methods. However, the trapezoid method obtained a statistically equal but slightly smaller values than the parabola.

Figure 4.15- Evolution of the BAI of two recaptured (within the same season) animals, with two different calculation methods. The first graph (4.15.a) showcases the individual 21Dr-010 and the second (4.15.b) 21Dr-011

The graphs above depict the increase of the BAI within the same season of two recaptured individuals (Figure 4.15). Both individuals showed a slight increase of their BAI in a short amount of time. In less than one month both animals gained more than one magnitude.

The BAI was measured with two different methods; the parabola and the trapezoid, and the graphs clearly states that the trapezoid method gives a slightly lower result than the parabola method. A non-parametric (independent) two-samples Wilcoxon test (p-value=0.4018) confirmed that the two methods are obtaining a statistically equal result. The average deviation between the outputs of the two methods is 0.56.

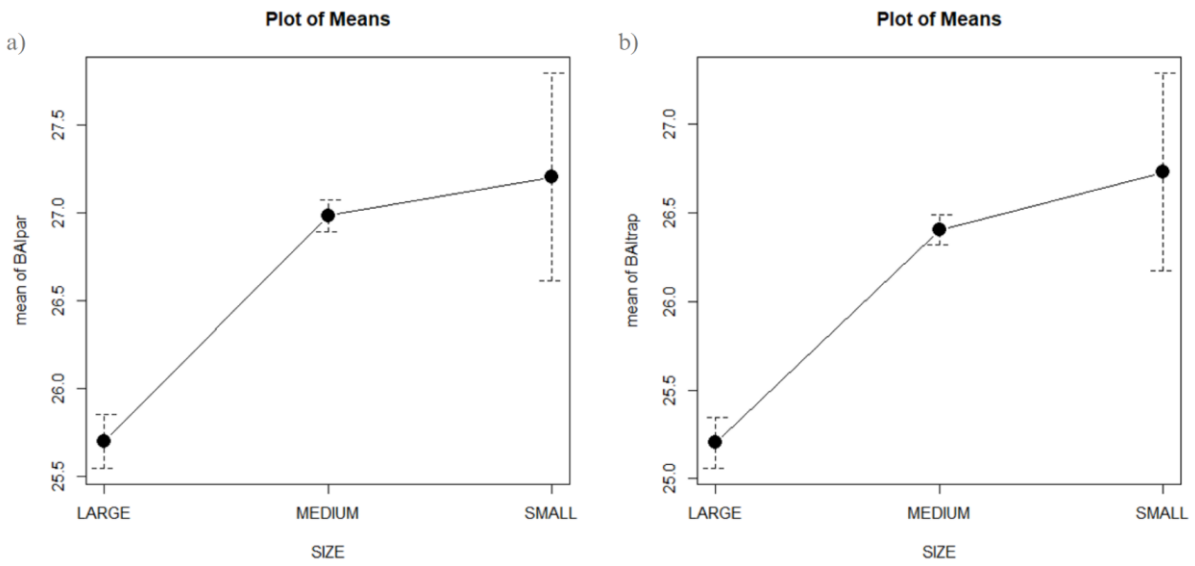

Figure 4.16- Plot of means representing the mean BAI of each size groups. Graph a) depicting the results from the parabola method and graph b) from the trapezoid, where the x axis is the size groups, and the y is the BAI measures

Figure 4.16 showcases variation of BAI measures (from both methods) according to size groups, where increasing body size negatively affects the BAI which with the growth simultaneously decreasing. Therefore, small animals obtain the highest BAI, but also this group has the highest variation of measures. The medium group has a slightly lower mean, with the lowest deviation. And the size group "LARGE" has the lowest mean of BAI. A non-parametric Kruskal-Wallis test confirmed (parabola method p-value: 0.0000002958, trapezoid method p-value: 0.000001053) that the means of BAI according to size groups are not statistically equal. The two graphs (Figure 4.16.a, b) represent the similarity of the two methods as both provides a statistically equal result, with only the difference of the trapezoid method constantly obtaining a slightly lower measure than the parabola.

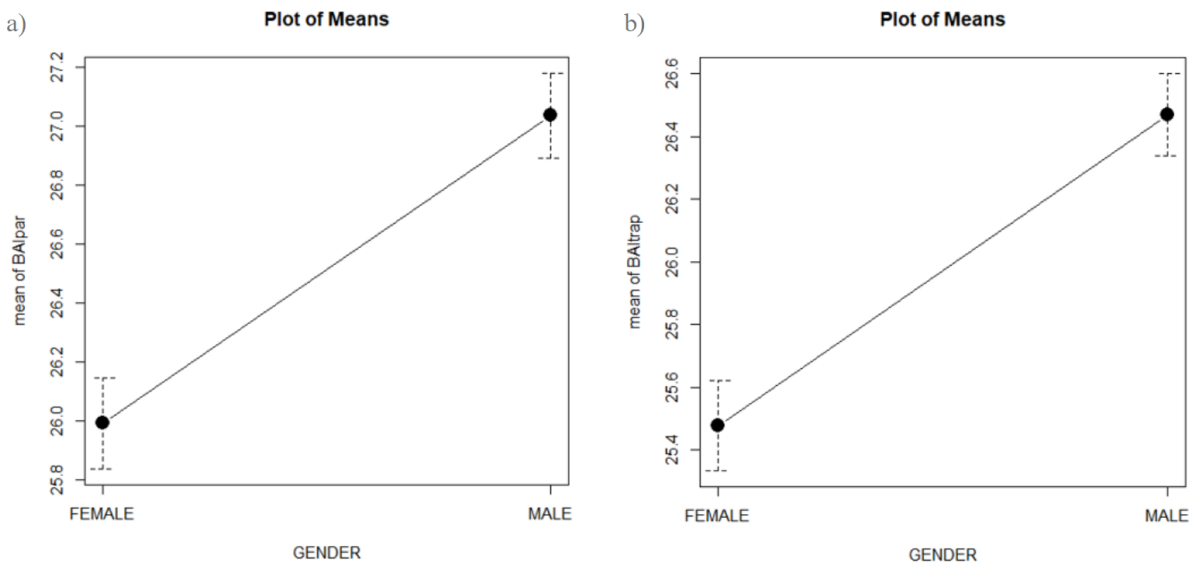

Figure 4.17- Plot of BAI means according to gender, where x axis represents the two sexes and the y axis is the BAI measures. Graph a) is the result obtained by the parabola method, and graph b) is the one obtained from the trapezoid method.

Figure 4.17.a, b depicts the differences of the mean BAI amongst the sexes. Both graphs demonstrates that in general males have a higher body area index than females. Furthermore, a non-parametric Kruskal-Wallis test was performed to test for potential significant differences existing between the BAI measurements among genders, and obtained the following results; parabola method p-value: 0.000001886, trapezoid method p-value: 0.0000002271, demonstrating that the sexes are not statistically equal with neither of the methods.

Moreover, the graphs again clearly show the similarity of the results from the two different methods, where the trapezoid obtaines a negligibly lower results.

4.2.6 BV evolution

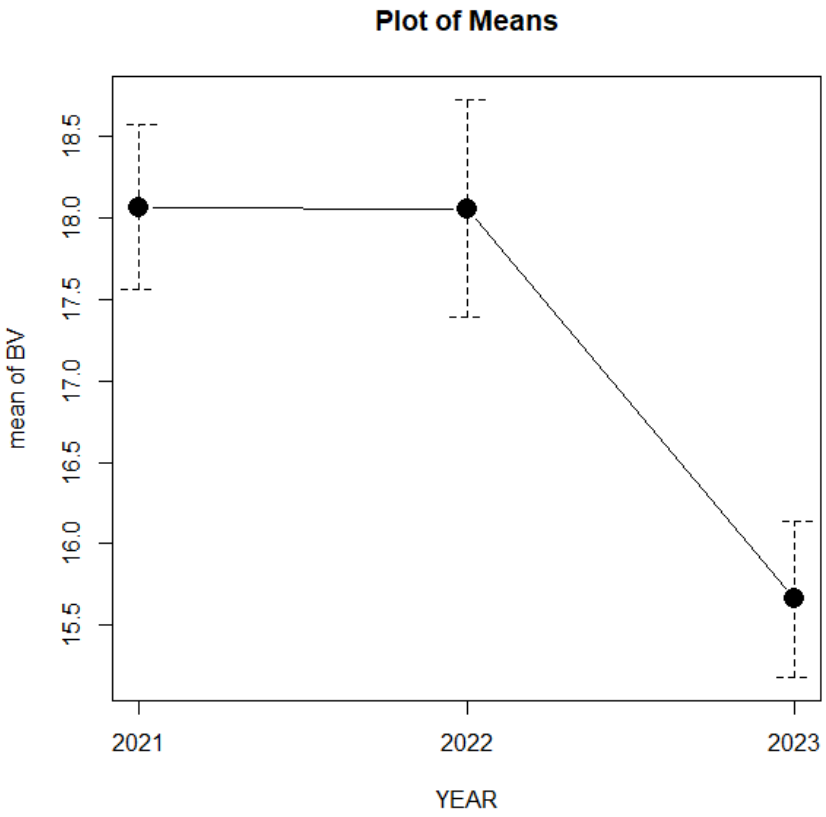

Figure 4.18- Seasonal variation of average BV between 2021 and 2023

Figure 4.18 depicts the mean BV for each studied year. It is clear from the graph that in 2021 and 2022 the mean Body volume was higher with 2.5 magnitudes. In comparison 2023 the whales obtained the lowest body condition. On these results a non-parametric Kruskal-Wallis test was run, which obtained a p-value of 0.02934. Indicating that the means of the BV are not statistically equal within the years.

The three graphs in Figure 4.19 depicts the BV evolution within the same foraging season of three individuals. Figure 4.19.a portrays the individual 21Dr-010, which whale was sighted in 2021 firstly in March than in May, during this time intervall the animal's BV expanded with 1.71 m³. The whale from the figure 4.19.b (21Dr-011) was sighted within a month in 2021 and gained 1.14 m³ during that time. And whale 22Dr-019 on figure 4.19.c was encountered in 2022 with only two days between the recaptures the individual showed an increase of its BV with 0.17 m³. The mean BV gain rate was 0.05 m^3 per day, within the seasons. This result is not representative due to the small sample size.

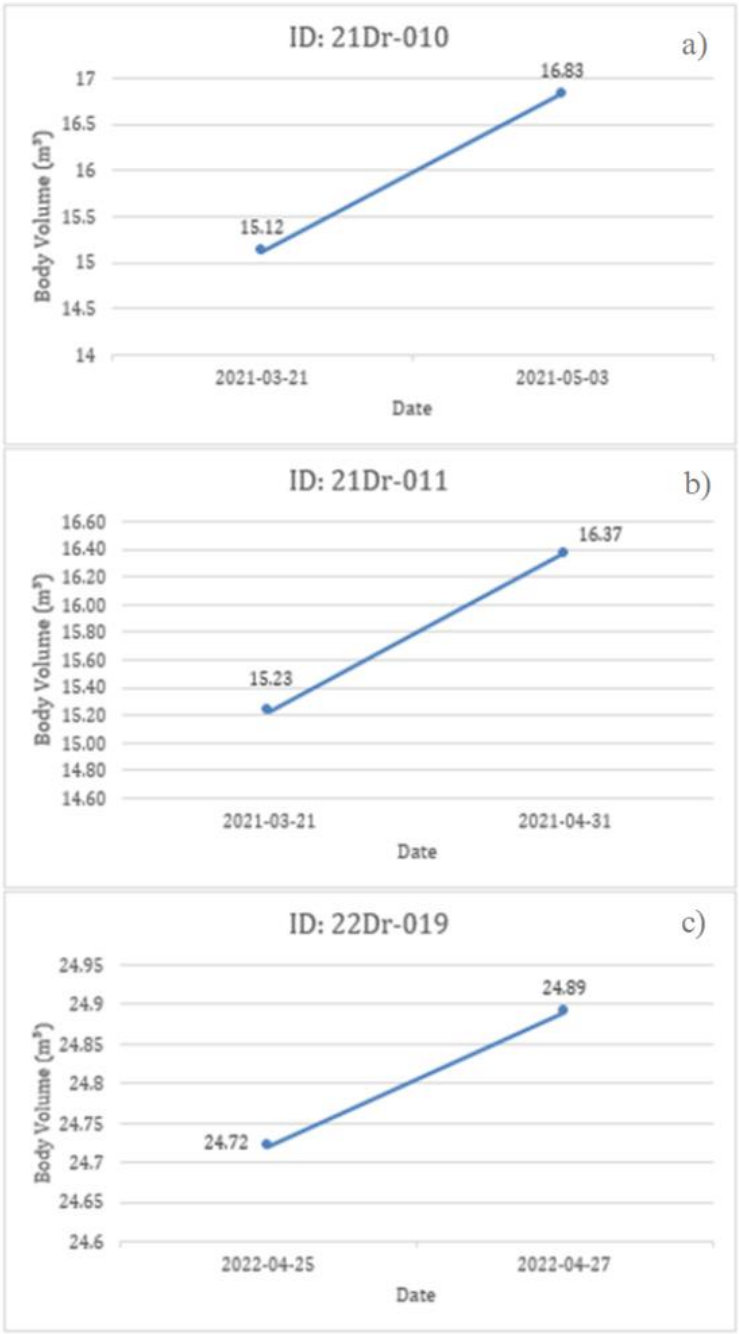

Figure 4.19- Linear charts of the BV evolution of three individuals that were recaptured within the same foraging season; on figure 4.19.a 21Dr -010, on figure 4.19.b 21Dr-011, and at last on figure 4.19.c 22Dr-019. The x axis represents the date when the animal was encountered and the y axis containes the BV in m^3.

5. Discussion

This thesis project was carried out based on the application of drone-based quantitative photogrammetry technique (Soledade *et al.*, 2020) to be able to assess the body morphology of the fin whale population in the Garraf coast, during three consecutive foraging seasons (2021-2023).

5.1 Challenges in obtaining body parameter measurements

Obtaining appropriate footage of cetaceans, in this case of fin whales is arduous, as there are several factors that affect it. Including the body position of the animal, as due to the movement the animal can be curved or arched or angled (not parallel with the sea surface) (Castrillon & Bengston Nash, 2020). The flippers proved to be one of the most problematic body parts to measure, due to its high number of potential orientations from which only a few is applicable in photogrammetry. Ratnaswamy & Winn (1993) earlier described this difficulty. Moreover, even if the animal is in the best position possible, the environmental conditions (glare, waves, turbulence, etc.) can mask the outline of the animal or parts of its body (Cheney *et al.*, 2022). Therefore, it was not possible to collect all desired body measures (TL, ETE, SB, SD, ASF, SPF, AFL, PFL, FS) (Ratnaswamy & Winn, 1993) from each photograph. The parameters which could be measured successfully in most cases were the following, in decreasing order: TL, SB, ETE and the FS.
This demonstrates that the most accessible measures are on the head. Based on this, in future studies the focus could be on these measures and comparative relations could be drawn between these main body parameters to leaser ones.

5.2 Growth trends

The Fin whales sighted in the Garraf coast within 2021 and 2023 of known sex showed constant difference of the total length between the genders, when females are larger than males, confirming the known sexual dimorphism within the species, what has been studied and declared by multiply authors including Aguilar & Lockrey (1986), Nortabar *et al.* (2003), Jefferson *et al*. (2015).

Based on the performed measurements the majority of the whales belonged to the “MEDIUM” size group and had a body size between 14 and 19 meters. This ratio stagnated during all three examined seasons (Figure 32.). This confirms Jefferson *e. al.* stated in 2015, which was that fin whales tend to grow smaller in the Northern Hemisphere. Furthermore, the animals that gathering in the area to forage are most likely a mixture of individuals from the Mediterranean populations and from the Atlantic population (Castellote *et al.*, 2012; Tort *et al.*, 2022). The two groups might have different growth tendencies, and it has been hypothesized by EDMAKTUB that in the Mediterranean fin whales reach shorter body length compared to the oceanic ones.

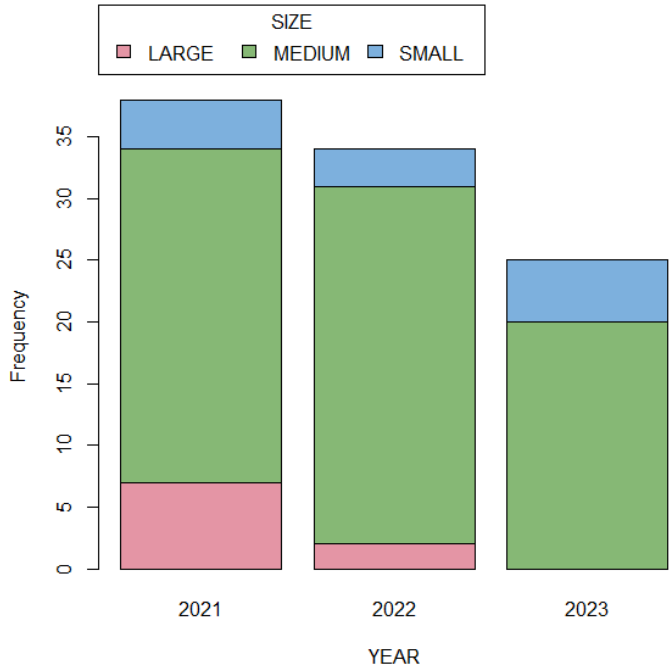

Figure 5.1- Bar chart of the size distribution (small, medium, large) amongst the three consecutive foraging seasons.

Individual growth demonstrates that based on the length variation between the foraging seasons the animals have grown within these few years (Figure 4.13). Giving an insight of the growth rate, which was an average of 1.4 meters/year. Aguilar *et al.* in 1987 stated that fin whales exhibit perpetual growth, which proves this result. Based on the results the animals from Figure 4.13.b and c belong to the same size group ("MEDIUM") and showed similar growth tendencies over time, between recaptures. In comparison, animal 21Dr-017 (Figure

4.13.a) is in the size range “LARGE” and displayed a slower growth rate per year, than the previous two. Indicating that the growth rate varies between genders and size groups. Which is suggested in other articles as well, including the previously mentioned one by Aguilar *et al.* where the authors refer to the postnatal period, as the time of the most accelerated growth, during which time the animal belong to the “SMALL” size group. However, due to the non-adequate aerial footage, difficulties arise as not all the resighted animals could have been measured and taken into account for this study. Therefore, between the three examined foraging seasons in the Garraf coast only a few (3) individual fin whales were used to obtain this result. Hence it is not a representative as it was based on an exceptionally low sample size. Subsequently, a larger dataset is required to draw statistically supported conclusions upon the growth of fin whales in the Garraf coast area.

The relation between different body parts provides a growth trend comparison which demonstrates that not all areas of the body grow simultaneously, certain parts grow in different times at different rates, which can vary between size groups and gender, this was also concluded in Ratnaswamy & Winn’s article of fin whales in 1993 and Bando et al., also obtained similar results on bryde’s whales from 2017.

Significant relationship was found in case of the ETE and the TL, however in comparison their growth tendencies differ depending on the group sizes and genders (Figure 4.6). At animals belonging to the “SMALL” size group the longitudinally growth of the body is dominant over the transversal growth of the head, Ohsumi has discovered in 1986 that growth of young animals is prioritized to reach larger size which achieves higher survival rates and earlier sexual maturity. After reaching 14 meters length, in the “MEDIUM” size group, the transverse growth of the head is better expressed and peaks, until the body length reaches approximately 19 meters, however the longitudinal elongation is still the primary. Thereafter, the transversal growth decreases to a minimal rate, while the total length is still increasing gradually in the “LARGE” size group. Subsequently, reaching a certain body size (approximately 14 meters) induces the growth of the ETE, after which the opposite effect takes place when the TL is about 19 meters the ETE transversal growth ceases. This result also indicates that the skull stops growing before the animal reaches its final length. There are corresponding records to these results in Fujino’s report upon body proportions of fin whales caught in the North Pacific from 1954 and also upon bryde’s whales by Bando *et al.* from 2017. In the study of Fujino described identical growth relation between the proportion of the head to the total length of the animals. Particularly that, the width of the head increases during the first body elongation period, and it

has its maximum growth rate when the animal gets to approximately 18-19 meters (which in our case is within the “MEDIUM” size group) and afterwards the growth tendency of the transversal growth of the head decreases in comparison of the growth rate of the total length (Ratnaswamy & Winn, 1993; Bando et al., 2017).

Regarding the genders there is a shift between the proportions of the ETE and the TL approximately at the body length of 14.5 meters. Under this size males obtain a narrower ETE distance, whereas above this body length males have a substantially wider ETE distance compared to their body length. While females displayed the opposite, as under 14.5 meters length they obtain wider ETE and as they increase in size the width of the head decreases in comparison. Consequently, fin whale population in the area shows a strongly expressed sexual dimorphism based on the proportions between ETE and TL, which expresses even more after reaching 15 meters length. Due to the width-length relations, where females are longer but narrower and males are shorter but wider in the eye-to-eye distance.

Withal, due to the masking environmental conditions and the position of the animals on the footage it was not possible to measure both of these variables (TL, ETE) on each still image. Therefore this result was based only on a small number of samples; 28 animals with known gender (9 males, and 17 females). Accordingly, further research is necessary to be statistically corroborated.

Regarding other proportionally related body parameters the gender is less or not influential (Bando *et al*., 2017). For example, in case of the AFL compared to the TL only the group sizes obtained significant relation between these body measures (Figure 4.9). The flipper length of “SMALL” and “LARGE” whales is considerably small to their body size, while “MEDIUM” sized animals have more variation, which likely arises from the larger deviation of the total length itself. In general, whales belonging to the “MEDIUM” size group have considerably larger flipper in comparison of the total length, then the other two groups (Figure 4.10). This result states that, the animals have the same proportions between the AFL and the TL at first stage of their life, when a longitudinal growth (TL) takes place and at the last stage when the final length is reached (based on body size). During these two stages the growth of the flipper is minimal, while in between, when the animals are “MEDIUM” sized the elongation of the flipper is best expressed, and the AFL proportionally caches up to the increasing TL of the body. In general, the animals have proportionally matching flipper size to their body size and, the flipper shows continuous growth throughout the whole lifespan.

Moreover, between the AFL and the FS only the size groups attained significant relation as a result. Within the "SMALL" size group the transverse growth of the fluke is dominant over the elongation of the flipper, while this trend changes in the "MEDIUM" group growth of the fluke decreases and the growth of the flipper increases, while in "LARGE" animals the growth of the fluke stagnates while the flipper continues to elongate (Figure 4.11). Substantially, the growth of the fluke is more advanced in smaller (likely younger) animals, probably due to its importance in the mobility of the animal (Bando *et al.,* 2017). And this growth shows decreasing tendency as the whale reaches larger body size. Whereas the elongation of the flipper is secondary compared to the fluke spread throughout, and it has a delayed development in comparison (Ratnaswamy & Winn, 1993). Furthermore, proportionally, smaller animals have smaller flippers related to the fluke, while "MEDIUM" and "LARGE" whales have larger flippers, between which the difference is minimal. Confirming the previously explained growth trends. However, in general the anterior flipper length related to the fluke spread is constantly around 0.5 and 0.6 to 1 (Figure 4.12).

In conclusion, the outputs display that there is variation among growth rates of certain body parts over time which highly depends on the length of the whole body (elongation rate), and therefore differs amongst size groups and sexes, similarly to Ratnaswamy & Winn's results. The examined body parts reach their maximum value during the time when the animal is between 14 to 19 meters of length ("MEDIUM" size group). Fujino (1954) has drawn a connection between the timing of the body proportions reaching their maximum and the sexual maturity of the individuals (Bando *et al*., 2017; Ratnaswany & Winn, 1993; Soledade *et al.,* 2020), however during this project it was not possible to confirm this.

These results demonstrate the utility of morphometric measurements to detect, quantify and assess the growth rate of individual animals and the potential to project it to the entire population (Dawson *et al*., 2017; Castrillon *et al*., 2020; Aoki *et al*., 2021; Cheney *et al.*, 2022; Degollada *et. al*., 2023; Durban *et. al.*, 2016). Moreover, the timing of the growth of specific body parts can be studied, which could give an insight of the age, sexual maturity, or other life history traits of the animal (Soledade *et al*., 2020; Aoki *et al.*, 2021).

5.3 Assessment based on width measurements

5.2.1 Body Volume

The body volume is an indicator of the nutritional status of cetaceans, the BV variation can reduce or increase body size and therefore the survival rate (Lockyer, 1986; Christiansen *et al*., 2019; Castrillon & Bengtson Nans, 2020; Soledade *et. al.*, 2020; Aoki *et al*., 2021; Hirtle *et al*., 2022). The results from the BV measures revealed differences of the productivity levels of the three examined seasons and connected to that the relative foraging success and energy replenishment of the incoming whales (Lockyer, 1986; Castrillon & Bengtson Nash, 2020). The deviation between the means of BV per year displayed that 2021 and 2022 was a very productive year and provided high foraging success of the animal, where they reached higher BV measures. But in contrast 2023 was a poor season, with low productivity and prey availability, therefore the whales could not accumulate perhaps the adequate amount of fat reserves like in the previous years (Figure 4.18). The body volume measures obtained variation of approximately 2.5 magnitude difference between the good years (2021, 2022) and the poor foraging season of 2023. This outcome confirms the other research line (behavior, distribution, zooplankton sampling etc.) results EDMAKTUB had accumulated throughout these three years, and it is representative to the difficulties of the season 2023, during which there were much less fin whale sightings and the whales showed different behaviors (such as travelling, resting) other than feeding (only 3 confirmed encounters).

The individual resighted animals within the same season showed relative increase of their body volume, with a BV gain rate of 0.05 m3 per day. Two of these measured recaptures were from 2021 and one from 2022, both of which seasons are considered “good”. But no data upon BV change was obtained from the considerably “bad” season in 2023, due to the low number of recaptures. Perhaps, because the animals did not stay in the same area as the prey availability was low and scattered, therefore could not accommodate several animals, thus most of the whales kept moving in search of food.

Due to the low sample size and to the missing data of genders no assessment was performed of the seasonal changes of the body volume between size groups or sexes. Notwithstanding, that no difference was found across age groups, genders, reproductive status in fin whales or among other species, such as humpback whales (Aoki *et al*., 2021). This is likely due to the general importance of the accumulation of sufficient energy storage for survival, as the energy demand is not only related to certain attributes of the animal such as age or size,

neither only to reproduction (Durban *et al*., 2016; Castrillon & Bengstone Nash, 2020; Soledade *et al*., 2020; Aoki *et al*., 2021).

5.2.2 Body Area Index

The individual BAI growth within and across seasons indicates relative foraging success and the accumulation of energy reserves of the measured whales (Lockyer, 1986; Castrillon & Bengtson Nash, 2020; Soledade *et al*., 2020). Resighted individuals within 2021 displayed general improvement of their BAI as the foraging season progressed within a considerably small amount of time (one month), this suggests that the animals spent most of their time feeding (Figure 4.15). Which also indicates that there was an appropriate amount of prey in the area, confirming the importance of the Garraf coast foraging ground (Tort *et al*., 2022). The individual from Figure 4.14, gained mass based on its BAI with one magnitude over three years. This result proposes, that during the three foraging seasons the whale was able to feed successfully enough to gain and adequate amount of energy reserve for the periods of migration and reproduction (Durban *et al*., 2016; Castrillon & Bengstone Nash, 2020; Soledade *et al*., 2020; Aoki *et al*., 2021). Furthermore, there is a high possibility that this individual did not use all its reserves in the meantime, as it did not just regained its reserves but further increased them. However, this result excludes short term deviations. Nonetheless, the BAI index can deviate to both negative and positive direction based on several external and internal factors within considerably short time periods (Soledade *et al*., 2020; Hirtle at. Al., 2022). Therefore, it would be more representative with data from both foraging and reproductive season or in a monthly basis.

The mean BAI measures showed variation amongst size groups and genders (Lockyer, 1986; Soledade *et al*., 2020). There is a significant difference between size groups, presenting the highest BAI within the “SMALL” size group and the lowest amongst “LARGE” animals. The size group “MEDIUM” has slightly lower BAI measures than the “SMALL” group. However, the BAI of the “LARGE” size group is drastically lower than the other two. Consequently, as the body size increases the BAI decreases simultaneously, especially above 20 meters body length. Demonstrating that young animals have a better body condition with higher fat reserves, which might be gained by lactating or the remains from lactation. And older animals with a large body size, which are mainly females have the least reserves, these animals might be recovering from pregnancy and lactation (post-weaning) (Lockyer, 1986; Soledade *et al*.,

2020). Furthermore, difference was found between the BAI means of genders (Aoki *et al.*, 2021), as the statistical analyses (non-parametric Kruskal-Wallis test) demonstrated that the sexes were not statistically equal. Males displayed higher BAI measures with one magnitude than females. This result might arise from the high energetic investment of females in reproduction (Lockyer, 1986), which causes high volume changes of the body (Soledade *et al.*, 2020), while the males obtain a more constant body state. There is a strong connection between these results, as according to both, gender, and size (Castrillon & Bengtson Nash, 2020; Aoki *et al.*, 2021) draw the conclusion that larger, probably older, mature females that likely invested in reproduction already have lower BAI measures. Similar findings were obtained of gray whales in the North Pacific by Soledade *et al.* in 2020. In this paper the authors conclude that gray whale calf obtains the highest BAI measurements, thereafter pregnant females and the lowest index was related to females in the period of lactation and after weaning (Soledade *et al.*, 2020).

Both the parabola and the trapezoid BAI calculation methods proved to obtain the consistently same results, as no remarkable difference was recognized on the whole number of measurements. Therefore, both are adequate to be applied, with only a small deviation between them, where the trapezoid obtains a slightly lower result than the parabola. Due to this difference the two methods can be used simultaneously to validate each other (Aoki *et al.*, 2021).

This study confirms Brunett *et al.* (2019), Soledade *et al.* (2020) and Aoki *et al.* (2021), who state that the body area index and the body volume can be confidentially applied to monitor energy reserves and body condition of free ranging cetacean (Aoki *et al.*, 2021) such as fin whales. Based on width measurements of the external body shape of the whales and it allows comparison across time periods and provides insight of the productivity of the environment, as the body condition is strongly linked to the prey availability (Cheney *et al.*, 2022). With a larger dataset long-time monitoring could provide insight of the seasonal variation of BAI, BV evolution. Therefore, I recommend continuing the collection of body width measures each foraging season in the Garraf coast.

5.3 Conclusion and future directions

Drone based photogrammetry proved to be a precise method to monitor the growth trends and body condition changes (Soledade *et al.*, 2020; Aoki *et al.*, 2021) of fin whales in the Garraf coast, to reduce uncertainties of nutritional status and body development. It was an important feature of the study to link individual whales to measurements obtained from photogrammetry (Cheney *et al*., 2022), which allowed monitoring changes in the body parameters over time (Durban *et. al.*, 2016).

However, it was only possible in the case of six animals, due to difficulties of adequate footage collection and time limit, regardless of the method. Nonetheless, all of these whales showed general increase in both growth and body condition (BV, BAI) assessment, from which the results were evenly distributed throughout the three examined year. Furthermore, inter-annual comparison of BAI measures provided insight of the productivity and into the carrying capacity of the area, showcasing the deviation in prey availability (Soledade *et. al*., 2020).

The results concerning body proportions confirm that there is a strong to moderate correlation between the growth rates of different body parts (Ratnaswamy & Winn, 1993; Bando *et al*., 2017; Soledade *et al*., 2020) among fin whales encountered in the Garraf coast. The variation of the strength of correlation represents the dependence between two anatomical regions (body parts). Besides, not all parts of the body develop at the same time neither with the same rate. Reaching certain length of the body induces or ceases the growth of specific areas. And even though there are general characteristics of growth trends, deviation can be found amongst size groups and gender.

Sex ratio and size distribution of the encountered fin whales in the Garraf coast are useful to improve the knowledge on population dynamics. Most animals that were within the study period were between 14 and 19 meters (“MEDIUM” size group) which indicates that the population mainly consist of young adults and mature animals.

Moreover, as these results help to fill in knowledge gaps upon the fin whale populations occurring in the Garraf coast, this technique has a potential to carry out long-term monitoring to accumulate data to be able to draw more reliable results upon the relation between body parameters, growth trends, changes in body conditions, and population dynamics (Durban *et. al.*, 2016; Dawson *et al*., 2017; Castrillon *et al*., 2020; Soledode *et al*., 2020; Aoki *et al*., 2021; Cheney *et al*., 2022; Degollada *et. al*., 2023). Which knowledge could be helpful to establish appropriate conservation and population management actions (Cheney *et. al*., 2022) to protect

the foraging ground within the area to maintain adequate food supply to the migrating fin whales (Christinasen *et al*., 2019; Soledade et al., 2020).

However, several difficulties were encountered while conducting this project, especially around the collection of adequate footage, mainly due to the unfavorable body position of the whales. I recommend the usage of the following whale parameters, which proved to be easier to collect; TL, ETE, SB, FS. Furthermore, there were several errors appeared when using distinctive features in the program MorphoMetriX and CollatriX, in the near future a second, improved version of both software will be released, which might be more sufficient to be used. Related to this, to address and mitigate uncertainties from altitude measurements a new software is under development by the Oregon State University to reduce the errors arising from this ambivalence and to improve the workflow.

Collaboration of research organizations would be beneficial to be able to collect (following the same protocol) and share more aerial footage from a larger study area, along the migration routes of the animals. Which would provide higher chances of recapturing animals, therefore short-term changes in individual body conditions could be monitored and it would provide more representative data of the hole population throughout each season. Based on these, even monthly comparisons could be drawn (Duran *et. al*., 2016; Castillon & Bentson Nash, 2020; Soledade *et. al.*, 2020).

Furthermore, if the animals belonging to the Atlantic or to the Mediterranean could be distinguished, the two population might show differences in their growth trends and in other attributes, which would be interesting to study.

6. Acknowledgement

The development of this study would not be possible without the support of EDMAKTUB Association, providing all the necessary equipment and platform to perform this project.
First and foremost, I would like to express my deepest gratitude to my co-supervisors from EDMAKTUB Association Beatriu Tort, who assisted and gave guidance throughout the whole process of this work.
Secondly, to Eduard Degollada PhD (president of EDMAKTUB Association) who explained the utility and different applications of drone-based research in cetacean studies and collected the footage that was used for this project.
Furthermore, I would like to thank Péter Tóth for his help in setting up MorphoMetriX and CollatriX, moreover for fixing the feature errors arising in MorphoMetriX.
Moreover, I would like to thank Anson Aguirre Firth for his support and for editing Figure 10.
And finally, I would like to thank my internal supervisor Catarina Vinagre PhD.

7. References

Aguilar A., & García-Vernet R. (2018). *Fin Whale. Wursig B., Thewissen J. G. M., Kovacs K. Encyclopedia of Marine Mammals, Third Edition, Academic press, Cambridge, Massachusetts. ISBN: 9780128043813, 368–371pp.*

Aguilar A., Lockyer C. H. (1986). *Growth, physical maturity, and mortality of fin whales (Baleanoptera physalus) inhabiting the temperate waters of the northeast Atlantic. Canadian Journal of Zoology, 65, 253-264pp.*

Aoki k., Isojunno S., Bellot C., Iwata T., Kershaw J., Akiyama Y., Martín Lopez L., Ramp C., Biuw M., Swift R., Wensveen P., Pomeroy P., Narazaki T., Hall A., Sato K., Miller P. (2021). *Aerial photogrammetry and tag-derived tissue density reveal patterns of lipid-store body condition of humpback whales on their feeding grounds. Proceedings of the Royal Society B: Biological Sciences, 288, 1-10pp.*

Bando T., Nakamura G., Fujise Y., Kato H. (2017). *Developmental Changes in the Morphology of Western North Pacific Bryde's Whales (Balaenoptera edeni brydei). Open Journal of Animal Sciences, 7(3), 344-355pp.*

Best P. B., Ruther D. (1992). *Aerial phtoogtammetry of southern right whales, Eubalaena australis. Journal of Zoology, 228(), 595-614pp.*

Bierlich K., Schick R. S., Hewitt J., Dale J. (2021). *A Bayesian approach for predicting photogrammetric uncertainty in morphometric measurements derived from UAS*

Marine Ecology Progress Series, 673, 193-210pp.

Burnett J. D., Lemos, L., Barlow, D., Wing, M. G., Chandler, T., & Torres, L. G. (2019). *Estimating morphometric attributes of baleen whales with photogrammetry from small UASs: A case study with blue and gray whales. Marine Mammal Science, 35(1), 108-139pp.*

Castellote M., Clark C., Lammers M. (2012). *Fin whale (Balaenoptera physalus) population identity in the western Mediterranean Sea. Marine Mammal Science, 28(2), 325-344pp.*

Castrillon J., Bengtson Nash S. (2020). *Evaluating cetacean body condition; a review of traditional approaches and new developments. Ecology and Evolution, 10(12), 6144-6162pp.*

Cheney B., Dale J., Thompson P.,Quick N. (2022). *Spy in the ksy: a method to identify pregnant small cetaceans. Remote Sensing in Ecology and Conservation 8(4), 492-505pp.*

Christiansen F., Sironi M., Moore M., Ricciardi M., Warick H., Irschick D., Gutierrez R., Uhart M. (2019). *Estimating body mass of free-living whales using aerial photogrammetry and 3D volumetrics. Methods in Ecology and Evolution, 10(12), 2034-2044pp.*

Dawson S., Bowman M., Leunissen E., Sirguey P. (2017). *Inexpensive Aerial Photogrammetry for Studies of Whales and Large Marine Animals. Frontiers in Marine Science, 4(), 366-373pp.*

Degollada E., Amihó N., O'Callaghan S. A., Varola M., Ruggero K., Tort B. (2023). *A Novel Technique for Photo-Identification of the Fin Whale, Balaenoptera physalus, as Determined by Drone Aerial Images. Drones, 7(3), 220-pp.*

de Oliveira L. L., Andriolo A., Cremer N. J., Zerbini A. N. (2022). *Aerial photogrammetry techniques using drones to estimate morphometric measurements and body condition in South American small cetaceans. Marine Mammal Science, 38(), 1-19pp.*

Durban J., Fearnbach H., Paredes A., Hickmott L., LeRoi D. (2021). *Size and body condition of sympatric killer whale ecotypes around the Antarctic Peninsula. Marine Ecology Progress Series, 677(), 209-217pp.*

Durban J., Moore M. J., Chiang G., Hickmott L. S., Bocconcelli A., Howes G., Bahamonde P. A., Perryman W. L., LeRoi D. J., (2016). *Photogrammetry of blue whales with an unmanned hexacopter. Marine Mammal Science, 32(4), 1510-1515pp.*

Fujino K., (1954). *On the Body Proportion of the Fin Whales (Balaenoptera physalus (L)) Caught in the Northern Pacific Ocean (I). Scientific Report of the Whales Research Institute, 9, 121-163pp.*

Gray P., Bierlich K., Mantell S., (2019). *Drones and convolutional neural networks facilitate auMethods in Ecology and Evolution, 10(9), 1490-1500*

Hirtle N., Stepanuk J., Heywood E., (2022). *Integraing 3D models with morphometric measurements to improve volumetric estimates in marine mammals. Methods in Ecology and Evolution, 13(11), 2478-2490pp.*

Hartman K., van der Harst P., Vilela R. (2020). *Continiouse Focal Group Follows Operated by a Drone Enable Analysis of the Relation Between Sociality and Position in a Group of Male Risso's Dolphins (Grampus griseus). Frontiers in Marine Science 7(), 283-pp.*

Jefferson T. A., Webber M. A., Pitman R. L. (2015). *Marine Mammals of the Word: A Comprehensive Guide to Their Identification, Academic press, Cambridge, Massachusetts. ISBN: 978-0-12-409542-7, 54-58pp.*

Lloret J., Palomera I., Salat J., Sole I. (2004). *Impact of freshwater input and wind on landings of anchovy and sardine in shelf Waters surrounding the Ebre (Ebro) River delta (north-west Mediterranean). Fisheries Oceanography, 13(2), 102-110pp.*

Lockyer C. (1986). *Body fat condition in northeast Atlantic fin whales, Balaenoptera physalus, and its relationship with reproduction and food resources. Canadian Journal of Fisheries and Aquatic Sciences 43(1), 142-147pp.*

Notarbar Tollo-di-sciar G., Zanardelli M., Jahoda M., Panigada S., Airoldi S. (2003). *The fin whale BAlenoptera physalus (L. 1758) in the Mediterranean Sea. Mammal Review, 44(2), 105-150pp.*

Ohsumi S. (1986). *Yearly change in age and body length at sexual maturity of a fin whale stock in the eastern north pacific. Scientific Reports of the Whales Research Institute, 37, 1-16pp.*

Shero M. R., Pearson L. E., Costa D. P., Burns J. M. (2014). *Improving the Precision of Our Ecosystem Calipers: A Modified Morphometric Technique for Estimating Marine Mammal Mass and Body Condition. PLoS ONE, 9(3), 91233-pp.*

Soledade Lemos, L., Burnett, J. D., Chandler, T. E., Sumich, J. L., & Torres, L. G. (2020). *Intra- and inter-annual variation in gray whale body condition on a foraging ground. Ecosphere, 11(4).*

Ratnaswarmy M., Winn H., 1993/2015. *Photogrammetric Estimates of Allometry and Calf Production in Fin Whales, American Society of Mammalogists, Vol. 74., No 2., 323-300pp.*

Rigual-Hernández A. S., Bárcena M. A., Sierro F. J., Flores J. A., Hernández-Almeida I., Snachez-Vidal A., Palanques A., Heussner S. (2010). *Seasonal to interannual variability and geographic distribution of the silicoflagellate fluxes in the Western Mediterranean. Marine Micropaleontology 77, 46-57pp.*

Tort Castro B., González R. P., O'Callaghan S. A., Dominguez Rein-Loring P., Degollada Bastos E. (2022). *Ship Strike Risk for Fin Whale (Balaenoptera physalus) Off the Garraf coast, Northwest Mediterranean Sea. Sec. Frontiers in Marine Science 9,*

8. Annex

```
Call:
lm(formula = logETE ~ logTL + GENDER, data = WHALE_BC)

Residuals:
      Min        1Q    Median        3Q       Max
-0.106233 -0.008490  0.005918  0.023073  0.105021

Coefficients:
               Estimate Std. Error t value     Pr(>|t|)
(Intercept)    -2.500363   0.093026  -26.88      < 2e-16 ***
logTL           1.126388   0.032260   34.92      < 2e-16 ***
GENDER[T.MALE]  0.047490   0.008077    5.88 0.0000000218 ***
---
Signif. codes:  0 '***' 0.001 '**' 0.01 '*' 0.05 '.' 0.1 ' ' 1

Residual standard error: 0.04834 on 167 degrees of freedom
  (279 observations deleted due to missingness)
Multiple R-squared:  0.8857,    Adjusted R-squared:  0.8843
F-statistic: 646.9 on 2 and 167 DF,  p-value: < 2.2e-16
```

Figure 8.1- Linear model of the logarithmically transformed variables eye to eye (ETE) and total length (TL) by gender

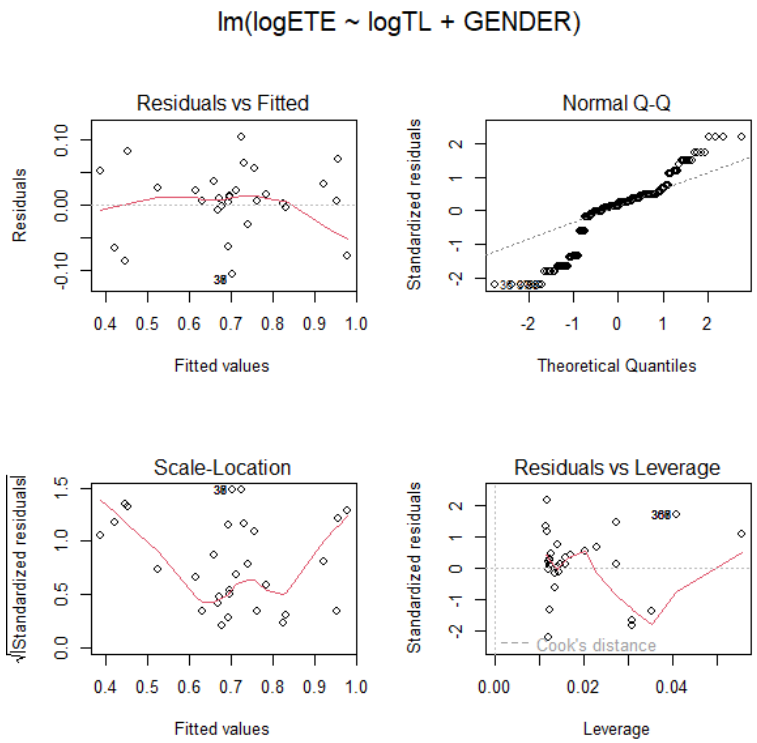

Figure 8.2- Diagnostic graphs of the residuals and fitted values of the previous linear model (ETE=TL+Gender)

```
Call:
lm(formula = logETE ~ logTL, data = WHALE_BC, subset = GENDER ==
    "FEMALE")

Residuals:
      Min        1Q    Median        3Q       Max
-0.109755 -0.057786 -0.000544  0.038392  0.103605

Coefficients:
            Estimate Std. Error t value Pr(>|t|)
(Intercept) -2.21051    0.13309  -16.61   <2e-16 ***
logTL        1.02571    0.04617   22.21   <2e-16 ***
---
Signif. codes:  0 '***' 0.001 '**' 0.01 '*' 0.05 '.' 0.1 ' ' 1

Residual standard error: 0.05851 on 85 degrees of freedom
  (261 observations deleted due to missingness)
Multiple R-squared:  0.8531,    Adjusted R-squared:  0.8513
F-statistic: 493.5 on 1 and 85 DF,  p-value: < 2.2e-16
```

Figure 8.3- Linear model of the logarithmically transformed variables eye to eye (ETE) and total length (TL) by gender, of the subset of female

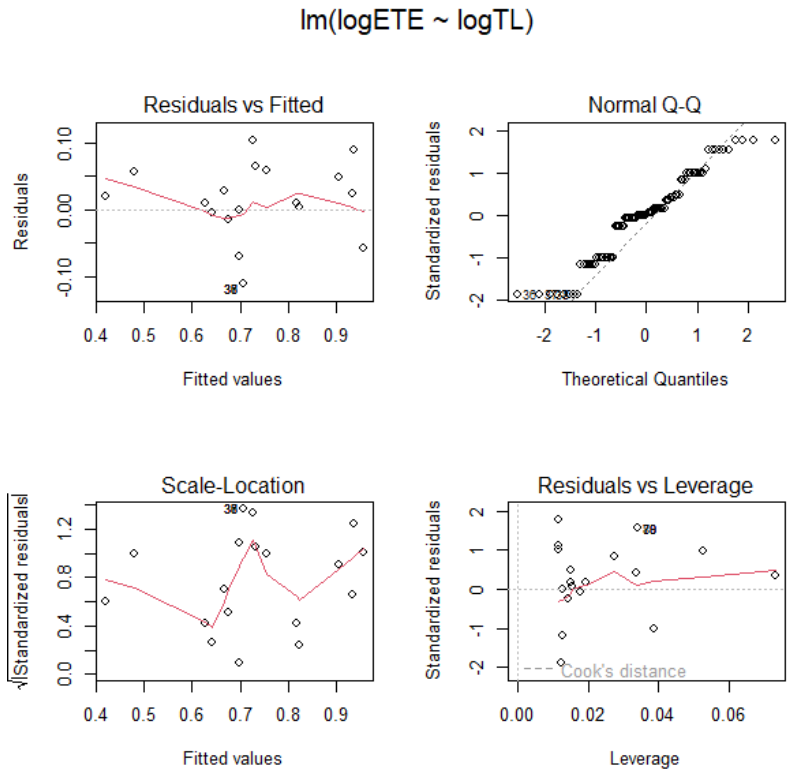

Figure 8.4- Diagnostic graphs of the residuals and fitted values of the previous linear model (ETE=TL+Gender==”Female")

```
Call:
lm(formula = logETE ~ logTL, data = WHALE_BC, subset = GENDER ==
    "MALE")

Residuals:
      Min        1Q    Median        3Q       Max
-0.043460 -0.007021 -0.001934  0.013884  0.060247

Coefficients:
            Estimate Std. Error t value Pr(>|t|)
(Intercept) -3.15565    0.07929  -39.80   <2e-16 ***
logTL        1.37919    0.02851   48.38   <2e-16 ***
---
Signif. codes:  0 '***' 0.001 '**' 0.01 '*' 0.05 '.' 0.1 ' ' 1

Residual standard error: 0.0228 on 81 degrees of freedom
  (263 observations deleted due to missingness)
Multiple R-squared:  0.9666,    Adjusted R-squared:  0.9661
F-statistic:  2341 on 1 and 81 DF,  p-value: < 2.2e-16
```

Figure 8.5- Linear model of the logarithmically transformed variables eye to eye (ETE) and total length (TL) by gender, of the subset of male

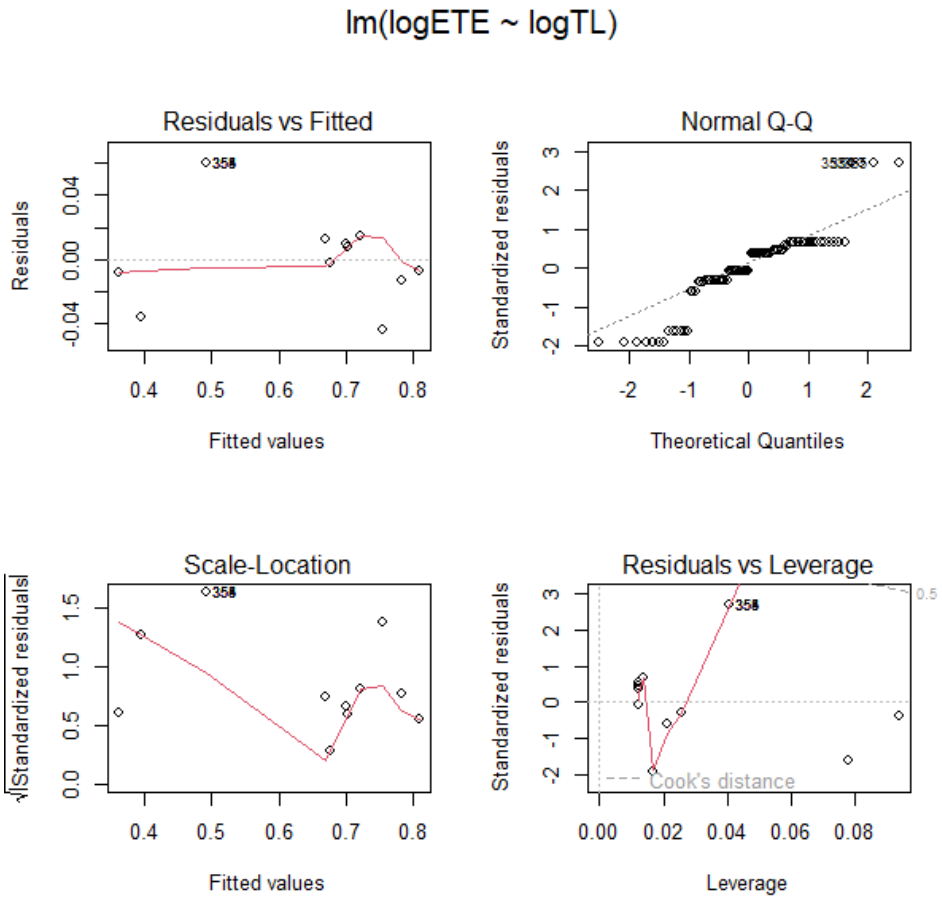

Figure 8.6- Diagnostic graphs of the residuals and fitted values of the previous linear model (ETE=TL+Gender==”Male")

```
Call:
lm(formula = logAFL ~ logTL + SIZE, data = WHALE_BC)

Residuals:
      Min        1Q    Median        3Q       Max
-0.170978 -0.034348  0.007111  0.047830  0.207895

Coefficients:
             Estimate Std. Error t value Pr(>|t|)
(Intercept)  -2.30513    0.17448 -13.212  < 2e-16 ***
logTL         1.01259    0.05644  17.941  < 2e-16 ***
SIZE[T.MEDIUM]  0.06458    0.02161   2.989  0.00310 **
SIZE[T.SMALL]   0.10457    0.03559   2.938  0.00363 **
---
Signif. codes:  0 '***' 0.001 '**' 0.01 '*' 0.05 '.' 0.1 ' ' 1

Residual standard error: 0.06662 on 233 degrees of freedom
  (212 observations deleted due to missingness)
Multiple R-squared:  0.7833,    Adjusted R-squared:  0.7805
F-statistic: 280.7 on 3 and 233 DF,  p-value: < 2.2e-16
```

Figure 8.7- Linear model of the logarithmically transformed variables anterior flipper length (AFL) and total length (TL) by size groups

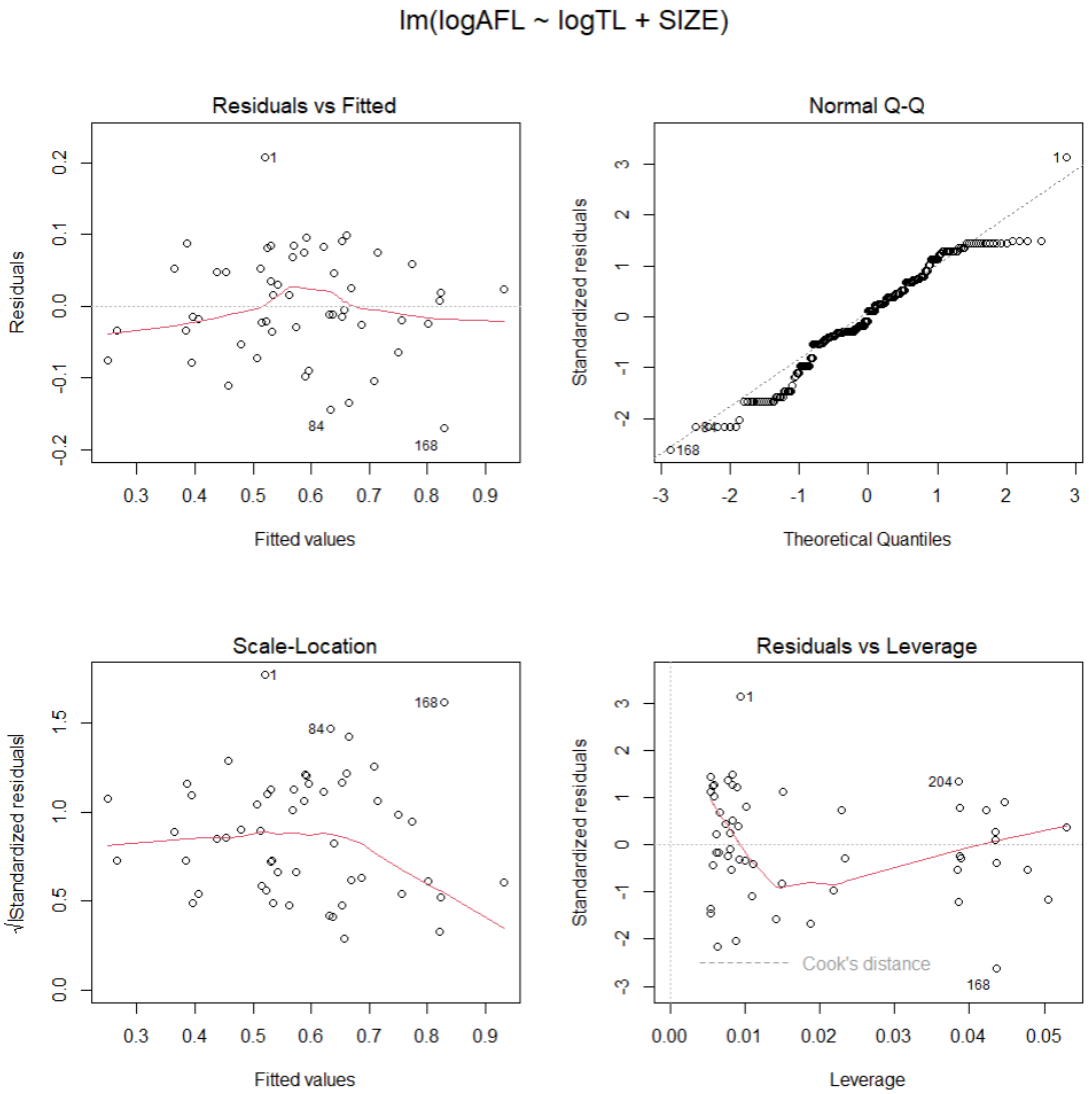

Figure 8.8- Diagnostic graphs of the residuals and fitted values of the previous linear model (AFL=TL+SIZE)

```
Call:
lm(formula = logAFL ~ logFS + SIZE, data = WHALE_BC)

Residuals:
      Min        1Q    Median        3Q       Max
-0.139955 -0.043765  0.009573  0.037008  0.139818

Coefficients:
              Estimate Std. Error t value    Pr(>|t|)
(Intercept)    0.03493    0.05411   0.646       0.519
logFS          0.53755    0.03479  15.451     < 2e-16 ***
SIZE[T.MEDIUM] -0.09457    0.01751  -5.401 0.000000203 ***
SIZE[T.SMALL]  -0.24906    0.02361 -10.549     < 2e-16 ***
---
Signif. codes:  0 '***' 0.001 '**' 0.01 '*' 0.05 '.' 0.1 ' ' 1

Residual standard error: 0.05349 on 184 degrees of freedom
  (261 observations deleted due to missingness)
Multiple R-squared:  0.8193,    Adjusted R-squared:  0.8164
F-statistic: 278.2 on 3 and 184 DF,  p-value: < 2.2e-16
```

Figure 8.9- Linear model of the logarithmically transformed variables anterior flipper length (AFL) and fluke spread (FS) by size groups

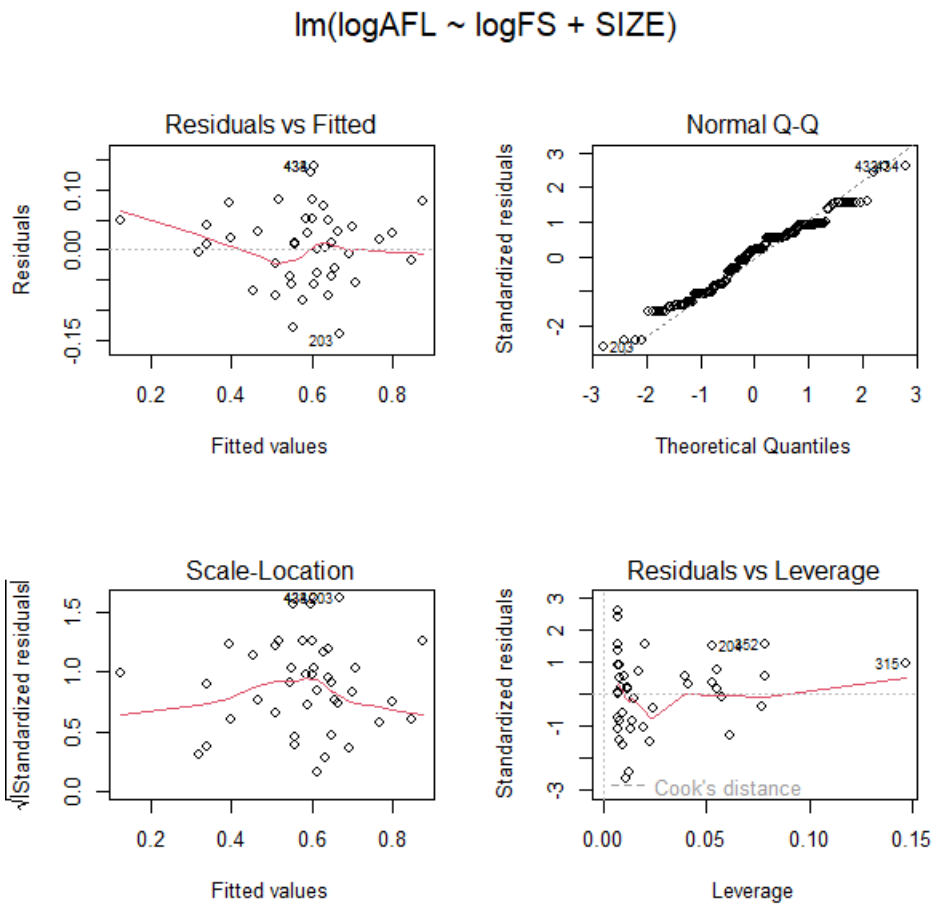

Figure 8.10- Diagnostic graphs of the residuals and fitted values of the previous linear model (AFL=FS+SIZE)